Iowa Water Center
Annual Technical Report
FY 2013

Introduction

The Iowa Water Center (IWC) represents a model of Water Resources Research Institutes that relies heavily on its 104(b) funding to carry out its charge of research, outreach and education related to Iowa's water. In FY2013, the substantial cut of 104(b) funds due to federal sequestration limited IWC activities in a noticeable way. However, IWC staff worked quickly and creatively to administer impactful activities in the face of budget cuts.

Water issues remain a critical research and education need in Iowa, particularly in the face of changing climate that results in extreme weather events. In FY2013, Iowa saw dramatic rainfall events in March, April and May that totaled 17.7 inches, nearly 7.5 inches above normal, which resulted in nearly 730,000 acres of row crops (corn and soybeans) not being planted. This rain caused flooding damage and soil erosion, implicating water quality issues in urban areas. These rains and the resulting consequences for water management, agriculture and Iowa economics guided IWC's efforts and interactions in FY2013.

In FY2013, after public input received in FY2012, officials in the state of Iowa released the Iowa Nutrient Reduction Strategy (NRS), available at nutrientstrategy.iastate.edu. The Iowa Water Center played a role in this document as Director Rick Cruse participated in development of the non-point source science assessment. The release of the NRS guided many of IWC's outreach efforts in 2013-2014, providing a commonality in which to connect consumers and organizations.

Iowa Water Center Director Rick Cruse returned for his 8th year in 2013-2014. Program Coordinator Melissa Miller completed one year of service in June 2013 and remains in the position. Dr. Cruse continued his service to the National Institute of Water Resources board as a regional representative. Continuity of staff in FY2013 allowed IWC to better refine processes to become efficient in their delivery of water resources research, outreach, and education.

Research Program Introduction

As in past years, the FY2013 Iowa Water Center research focus place particular emphasis on changes in climate patterns. The FY2013 call for proposals for the 104(b) program netted eight, extremely high-quality proposals related to water management in the face of climate variability. Ultimately, two projects were chosen for funding in FY2013: Quantifying Field Water Balance Components as Affected by Shifts in Land-Use Patterns: Implications for Minimizing Agricultural Impacts on Water Quality in Iowa (the second year of a 2-yr project), and Rainfall, temperature and discharge over Iowa: climate controls and seasonal forecasting. Unfortunately, the latter of these projects was eliminated during budget cuts due to federal sequestration. In addition, a special project funded by US Army Corps of Engineers through pass-through funds entitled "Hysteresis in Index-Velocity Rating Curves" was completed this fiscal year.

The Iowa Water Center also facilitated submission of three proposals to the 104(g) program: Development of a Comprehensive Hazard to Loss Modeling Framework for the Residential Damage Associated with Inland Flooding from North Atlantic Tropical Cyclones, A model for predicting the quantity and quality of water from collector wells, and Development of Design Specifications for a National Stream Morphology Database. Unfortunately, this program was not funded due to federal sequestration. IWC notified the submitting investigators in a timely manner and maintained very open communication to foster good relationships with the submitting institutions.

Quantifying Field Water Balance Components as Affected by Shifts in Land-Use Patterns: Implications for Minimizing Agricultural Impacts on Water Quality in Iowa

Basic Information

Title:	Quantifying Field Water Balance Components as Affected by Shifts in Land-Use Patterns: Implications for Minimizing Agricultural Impacts on Water Quality in Iowa
Project Number:	2012IA194B
Start Date:	3/1/2013
End Date:	2/28/2014
Funding Source:	104B
Congressional District:	Iowa 004
Research Category:	Water Quality
Focus Category:	Water Use, Water Quality, Water Quantity
Descriptors:	None
Principal Investigators:	Robert Horton, Matthew J. Helmers

Publications

1. Luo, C., Z. Wang, T. J. Sauer, M. J. Helmers, D. Sidhu and R. Horton. 2013. Evapotranspiration measurements in reconstructed prairie and row crop systems with a portable canopy chamber [Poster]. Soil Science Society of America annual meetings, Tampa, Florida.
2. Luo, C., Z. Wang, T. J. Sauer, M. J. Helmers, D. Sidhu and R. Horton. 2014. Evapotranspiration measurements in reconstructed prairie and row crop systems with a portable canopy chamber [poster]. Iowa Water Center Conference, Ames, Iowa.

Iowa Water Center Annual Report

1) Problem/Research Objectives

Increasing energy demands and concerns about climate change and fossil fuel depletion has led to an interest in alternative energy systems. Bio-fuel demand may increase in the future. Bio-fuel can be produced from food grain or from non-grain plant biomass. There are potential problems associated with converting plants into bio-fuel. One potential problem is the competition between food demand and energy demand. Another potential problem is that use of plant residues of annual crops may lead to accelerated soil erosion and environmental risk. Compared to annual row crops, perennial vegetation, such as prairie, may have some desirable qualities for use as a bio-energy crop. However, a landscape conversion to perennial vegetation under a climate change background may significantly influence regional hydrology and nutrient dynamics. Thus, the main problem addressed in this project is to quantify field hydrology, including water balance and water use by evapotranspiration, ET, of annual row crops, corn and soybean, and a perennial mixed prairie.

Specific objectives of this research project are as follows:

- To measure and contrast dynamic soil water storage, drainage and evapotranspiration in reconstructed mixed prairie and no-till corn and soybean cropping systems.
- To understand the relation between field water balance components and off-site water quality impacts of alternative cropping systems and management strategies.
- To use field data to evaluate and improve a crop hydrological and water quality model, and then use the model to predict implications of land use conversion on water quality and quantity for a variety of selected cropping systems, soils, and climatic conditions.

2) Methodology

<u>Plant Canopy ET-Chamber Design and Construction</u>**:**

Portable, dynamic canopy chambers will be used to measure ET from the different cropping systems. The chambers avoid microclimate restrictions and are usable in small scale plots where eddy covariance and Bowen ratio methods are not suitable.

The portable, dynamic canopy chambers were constructed of aluminum frame covered with Mylar film to allow radiation to enter. Three different size chambers were constructed: small, medium and large, to fit over plants at different crop growing stages. The chamber sizes are shown in Table 1.

Table 1. Chamber Sizes

	Length (m)	Width (m)	Height (m)
Small	1.52	1.00	0.61
Medium	1.52	1.00	0.95
Large	1.52	1.00	1.56

The sensors installed in the chamber are LI-7500 gas analyzer. It is used to measure vapor concentration and carbon dioxide concentration varies with time. The device makes 20 measurements per second. Each measurement sequence lasted for one minute, so each time the chamber was used 1200 data points were collected to calculate the ET flux and the net carbon dioxide flux. This project focuses on the measured ET-fluxes.

Installed both inside and outside of the chamber are thermocouples which measure the air temperature, barometers which measure the air pressure, infrared thermometers which measure the plant temperature, and quantum sensors which measure the solar irradiance. These sensors are used to document that there are similar ambient conditions inside and outside of the chamber. A CR 3000 datalogger is connected to chamber sensors in order to record the data. Chamber are shown in Fig. 1.

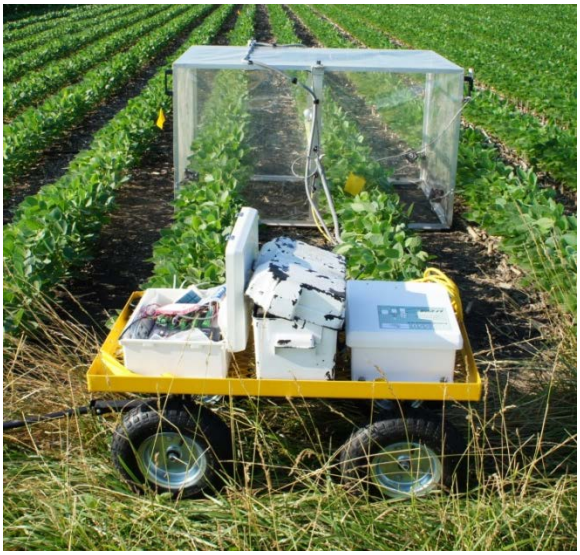

Fig. 1. Portable, dynamic canopy chambers are shown positioned in field plots.

Sampling Protocol:

The Comparison of Biofuel Systems (COBS) research site near Ames, Iowa was the field study site. It was established in 2008. There are 24 plots with 6 cropping systems. The research focus on corn in corn-soybean rotation, soybean in corn-soybean rotation and continuous prairie unfertilized system. Fig. 2 shows the COBS research site

Fig. 2 Comparison of Biofuel Systems (COBS) research site

In order to determine the water storage, five TE sensors (FDR sensor, Decagon Devices Inc.) are installed at different depths 5 cm, 10 cm, 18 cm, 30 cm, and 50 cm in each plot. The sensors are used to monitor soil water content and soil temperature throughout the growing season. Drainage and rainfall data are collected and used to calculate plot water balances.

In 2013, chamber measurements of maximum and average ET fluxes were made on 16 selected sunny days. Diurnal ET flux measurements were made on 2 sunny days (DOY 168, DOY 241).

Data Analysis

The chambers were manually positioned over the crops for a minimum amount of time to collect accurate flux measurements (60 seconds). Then chambers were removed to minimize chamber effects on light, wind speed, and air/leaf temperature. The CR 3000 recorded the vapor concentration and carbon dioxide concentration with time. Theoretically, those concentrations should increase linearly, and ET can be be determined from the slope of the line. We used an adaptive linear regression algorithm to calculate the slope of the linear trend and get the ET flux and carbon dioxide emission flux for each measurement period.

The chamber approach allows repeated measurements at multiple locations within the plot area, and the daily maximum and average ET flux can be determined. For diurnal measurements, a Fourier series is used to describe the trend of the diurnal evapotranspiration measurements.

Weather data were collected at the COBS site weather station. The Priestley-Taylor Equation used the weather station measurements to calculate potential evaporation at the site.

Plot water balance for each cropping system was calculated with the measured soil water contents, drainage, and rainfall. Rainfall was the input, water content change was change in storage, and the outputs were drainage and ET. Using plot measurements, ET was calculated as the residual. The water balance ET measurements were compared with the chamber ET measurements, and the measured ET values were compared with the potential ET calculations.

3) Principal Findings and Significance

ET-Chamber Measured Flux

Figure 3 provides one example of the ET-chamber measured water vapor concentrations with time. Indeed, the chamber provided data with a strong linear trend, and it was easy to calculate ET fluxes.

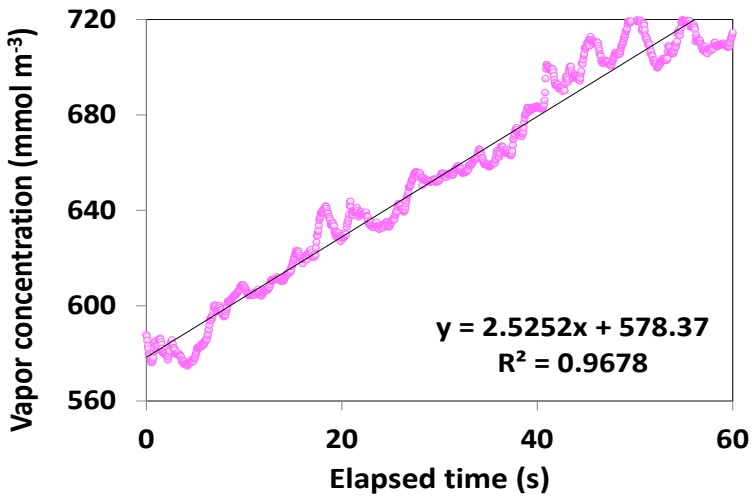

Fig. 3 ET-chamber measured water vapor concentrations with time.

ET-Chamber Measured Diurnal Fluxes in the Cropping Systems

Comparison of the diurnal ET fluxes among the three cropping systems showed that corn exhibited larger ET fluxes than soybean and prairie, and prairie had larger ET fluxes than soybean. The diurnal ET-curves in Fig. 4 contain flat tops, which may be

due to dry soil conditions. The dry soil conditions in 2013 limited actual ET in the cropping systems.

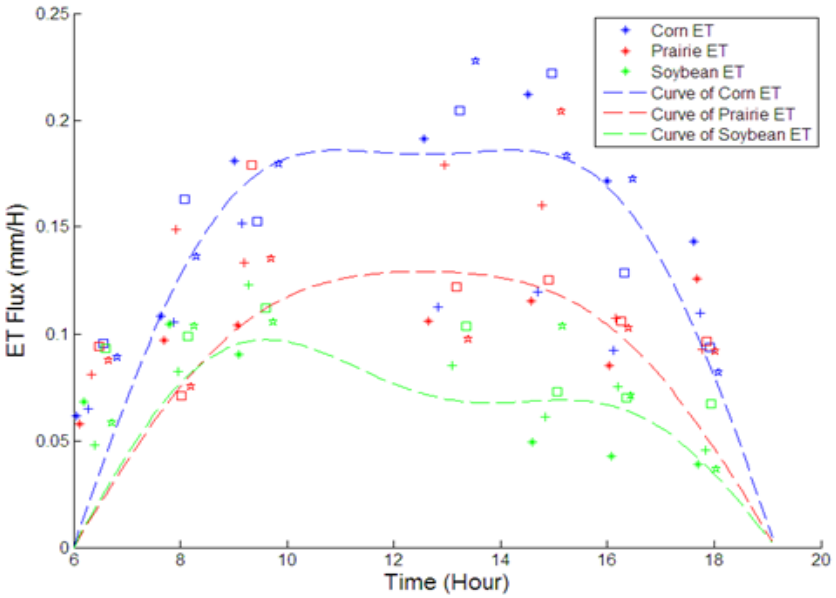

Fig. 4 Chamber measured diurnal ET fluxes in the cropping systems.

Seasonal Chamber ET, Water Balance ET, and Potential ET

Comparison of seasonal ET fluxes (chamber method and water balance method) with potential ET (Priestley-Taylor Equation) showed that for the 2013 dry growing season, the potential ET was larger than the actual ET due to limitations in the available soil water.

The water balance ET values were generally less than the chamber ET values, because soil water was measured only to a depth of 50 cm and plant roots may have extracted water from deeper soil (Fig. 5). Thus, the chamber ET data very reasonably compared with the water balance ET values.

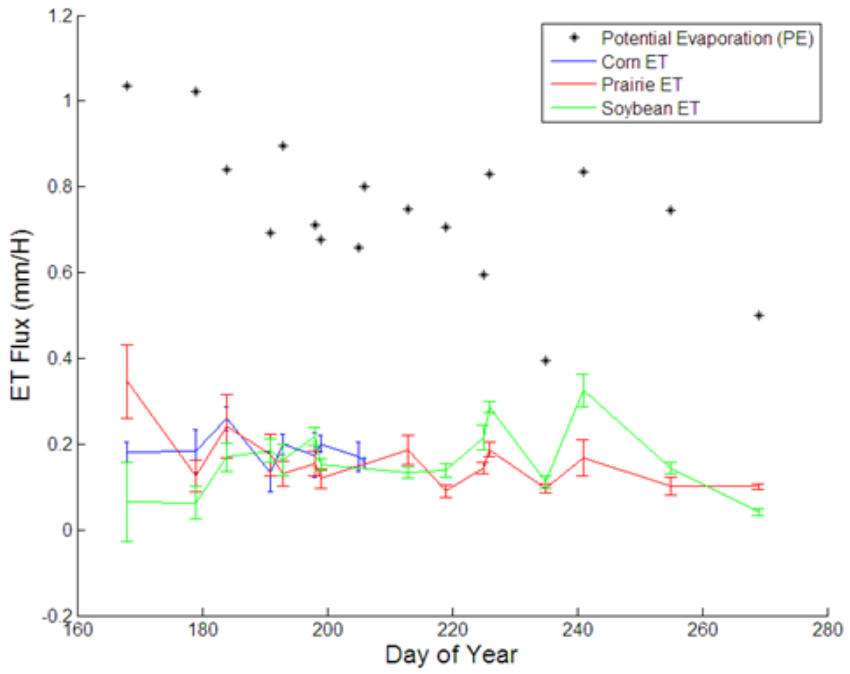

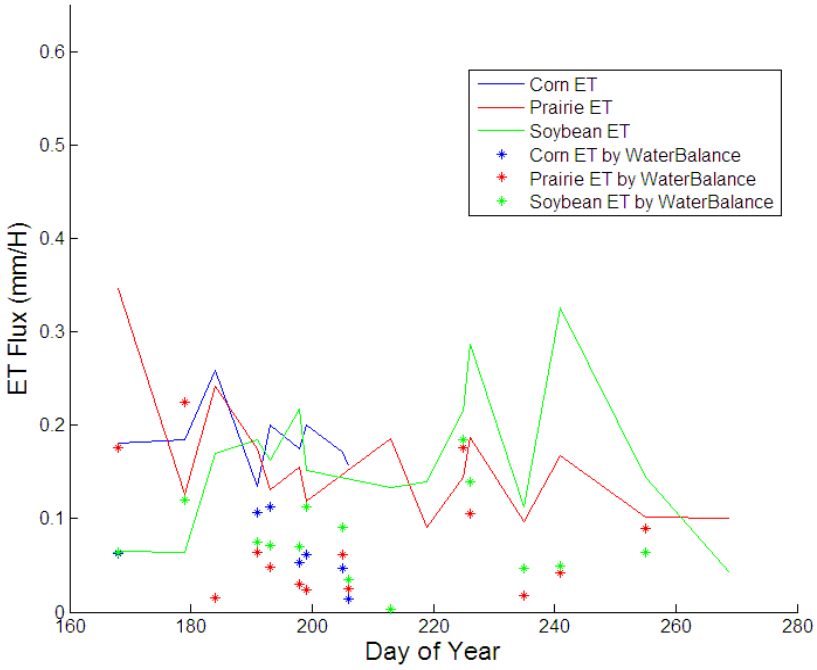

Fig. 5 The upper figure shows a comparison between potential evaporation and chamber ET, and the lower figure shows a comparison between water balance ET and chamber ET.

<u>Soil Water Contents Decreased During the Growing Season</u>

Figure 6 presents the precipitation and soil water content data during the 2013 growing season for the prairie and soybean plots. The decreasing trend of soil water content through entire season was due to the dry weather with relatively low

precipitation. Soil water content of the prairie field shows rapid decrease in the early season. The prairie matured earlier than corn and soybean. Prairie began to use soil water earlier than corn and soybean. Later in the growing season soil was relatively dry in the prairie while soil was wetter in corn and soybean. With low precipitation in 2013, the soil water contents exerted control on ET of the cropping systems. Early in the season the prairie had largest ET, while later in the season, due to larger water contents, soybean ET exceeded prairie ET.

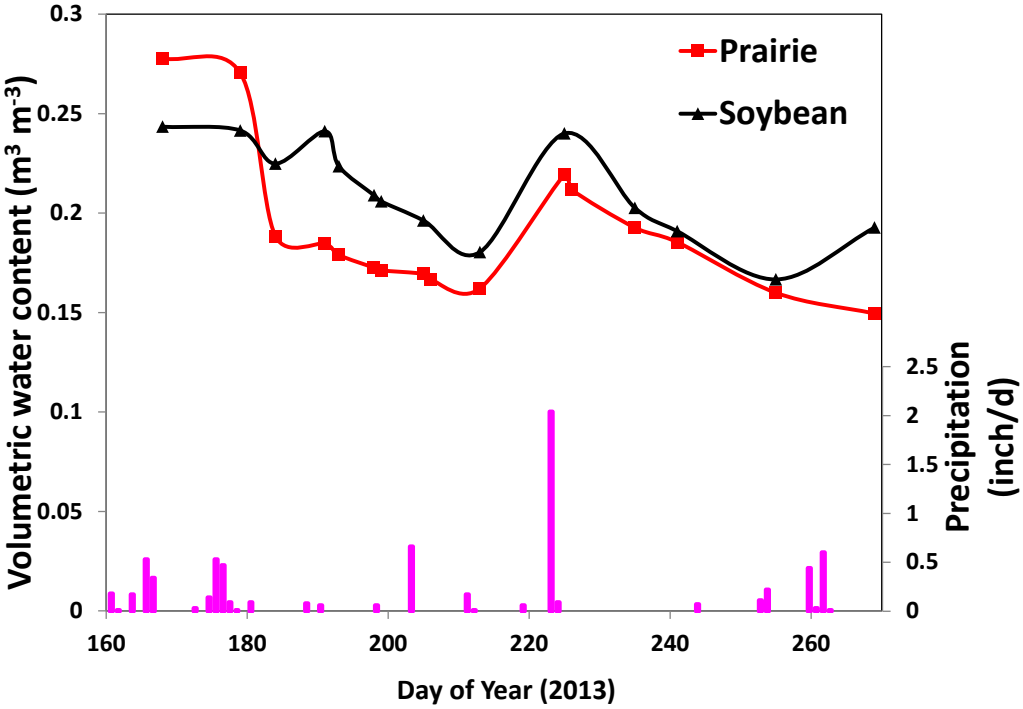

Fig. 6 Precipitation and Soil Water Content Data during the Growing Season

Significance

During the 2013 growing season, the evapotranspiration flux was measured on 18 different days, including 2 diurnal ET flux measurements. Chamber-ET values were compared with water balance values and potential evaporation. Based on the comparisons, it is clear that the portable canopy chamber provided reasonable estimates of ET flux for the different cropping systems. Thus, we have developed a new method for quantifying plot-scale ET fluxes of annual and perennial cropping systems.

4) Summary and Conclusions

ET from different cropping systems was quantified with the chamber measurements. Early in the growing season, ET fluxes in prairie were larger than in soybean. Late in the growing season, ET fluxes in soybean were larger than in prairie. Although measurements in only one cropping season do not provide conclusive information on

the long-term impacts of crop water use and regional hydrology, the results do help us understand the timing of crop water use in a dry year. Because of early growth and a long growth period, the prairie uses water early and causes the soil to dry out quickly which limits late growth opportunities. One preliminary conclusion is that soil water is needed for a longer period of time to meet the demands of prairie as compared to corn and soybean. This is important information to consider for rain-fed agricultural areas.

5) Listing of publications that have resulted from this research

Two posters of this research were presented. The posters had abstracts as well.

Luo, C., Z. Wang, T. J. Sauer, M. J. Helmers, D. Sidhu and R. Horton. 2013. Evapotranspiration measurements in reconstructed prairie and row crop systems with a portable canopy chamber. Soil Science Society of America annual meetings, Tampa, Florida.

Luo, C., Z. Wang, T. J. Sauer, M. J. Helmers, D. Sidhu and R. Horton. 2014. Evapotranspiration measurements in reconstructed prairie and row crop systems with a portable canopy chamber. Iowa Water Center Conference, Ames, Iowa.

6) Student support provided by this research

Graduate Students -- Devinder Sidhu and Zhuangji Wang were supported by Agronomy Department Endowment funds, and Chenyi Luo was supported in part on these project funds.

Undergraduate Student -- Jackson Griffith was supported by these project funds.

7) Achievements and awards for this research

None

8) Any additional funding this research has received

The research project was partially supported with USDA funds and Pioneer funds, and the required matching funds for the project were provided by Iowa State University Department of Agronomy Endowment.

Watershed scale water cycle dynamics in intensively managed landscapes: bridging the knowledge gap to support climate mitigation policies

Basic Information

Title:	Watershed scale water cycle dynamics in intensively managed landscapes: bridging the knowledge gap to support climate mitigation policies
Project Number:	2012IA215G
Start Date:	9/1/2012
End Date:	8/31/2014
Funding Source:	104G
Congressional District:	IA-2nd
Research Category:	Climate and Hydrologic Processes
Focus Category:	Agriculture, Hydrology, Water Quantity
Descriptors:	None
Principal Investigators:	Thanos N Papanicolaou, Keith Edwin Schilling, Douglas Schnoebelen, Christopher Wilson

Publications

1. Dermisis, D., A.N. Papanicolaou, B. Abban, and D. Flanagan. Dynamic approach for predicting soil transport and delivery from fields and small catchments to headwater streams: field experiments and analysis. Earth Surface Processes and Landforms. In Preparation (2014).
2. Papanicolaou, A.N., M. Elhakeem, C.G. Wilson, C.L. Burras, L.T. West, B. Clark, and B. Oneal. Understanding the variability of saturated hydraulic conductivity at the hillslope scale due to soil property heterogeneity induced by land management and erosion. Hydrological Sciences Journal. In Preparation (2014).

Title: Watershed scale water cycle dynamics in intensively managed landscapes: bridging the knowledge gap to support climate mitigation policies.
Sponsor Award/Grant #: G12AP20154
Annual Summary: March 1, 2013 to February 28, 2014
PI: A.N. Papanicolaou, Professor and Henry Goodrich Chair of Civil and Environmental Engineering, The University of Tennessee

1) Problem/Research Objectives

Our **overarching goal** for this project is to develop an integrative suite of established models to account better for the interplay between Land Use/ Land Cover (LU/LC) and climate on the water cycle dynamics in rapidly changing Midwestern landscapes at the watershed scale.

In this reporting period, we have used a Top-Down Approach with the Soil And Water Assessment Tool (or SWAT model) to identify critical sub-watersheds in terms of their contributions to flooding within the Clear Creek, IA watershed. We are currently using a Bottom-Up Approach with the Water Erosion Prediction Project (or WEPP model) to assess specific BMPs within these critical sub-watersheds and to quantify accurately the partitioning of surface and subsurface flow for assessing BMP efficiency.

2) Methodology

In this reporting period, water table monitoring wells were installed throughout Clear Creek to provide critical input data for the models used in this study. The modeling of the infiltration of water into the subsurface, especially in tile-drained areas, is strongly influenced by the depth of the water table and hence is a key parameter for both WEPP and SWAT. Thirteen water table wells up to 25 ft. in depth were installed in Clear Creek, some of the first of their kind in the area. Four wells were place along an agricultural hillslope (i.e., crest, shoulder, backslope, and toe slope), while three wells were placed along hillslopes in a grassed/ forested area, as well as on hillslopes in both suburban and urban areas. These wells are instrumented with pressure/ water level and temperature sensors. The sensors are set with a half-hour monitoring period and the data are collected monthly.

SWAT simulations were also performed. The version of SWAT used included tiles in the model code. SWAT was used to divide first Clear Creek into smaller sub-watersheds based on drainage patterns and then into Hydrologic Response Units representing combinations of current management practices, prevalent soils, and average slopes.

Finally, WEPP simulations were used to help determine the efficiencies of Alternative Tiles Intakes (i.e., modified rock filters with wood chips to facilitate denitrification) placed in Clear Creek. The model simulations utilized previously measured single rainfall events and design storms to determine the delivery of water and sediment to the Alternative Tiles Intakes. These results were also used to establish experimental conditions for laboratory studies. This modeling of the Alternative Tiles Intakes corresponds to previous simulations regarding other BMPs in Clear Creek, including grassed waterways.

3) Principal Findings and Significance

Figure 1A shows runoff volumes from the sub-watersheds in Clear Creek for the 100-year, 24-hour design storm. The highest runoff volumes were found in the upper parts of the watershed where agriculture was most prominent. Runoff volumes in the sub-watersheds decreased in magnitude as grasslands and forested areas increased in proportion relative to other land uses. The sub-watersheds in the central part of the watershed are covered in grassed and forested areas over more than half of their total acreage. Consequently, these watersheds had the lowest runoff.

The annual average runoff distribution in Clear Creek (Figure 1B), which was determined using SWAT shows the urban sub-watersheds in the eastern part of the watershed, which includes the city of Coralville, had the highest annual runoff in contrast to the agricultural areas, which had the highest runoff during the individual high magnitude events. This may be attributed to the impervious land cover of the urban areas, which prevents rainfall for all events (large and small) from infiltrating into the soil or being taken-up by vegetation. Thus, even the rainfall from small events was converted to runoff in urban areas causing total runoff volumes to increase over a year. The predominantly agricultural sub-watersheds still had high annual runoff volumes, while the sub-watersheds in the central part of the CCW, which have more grasslands and forested areas, had the least annual runoff.

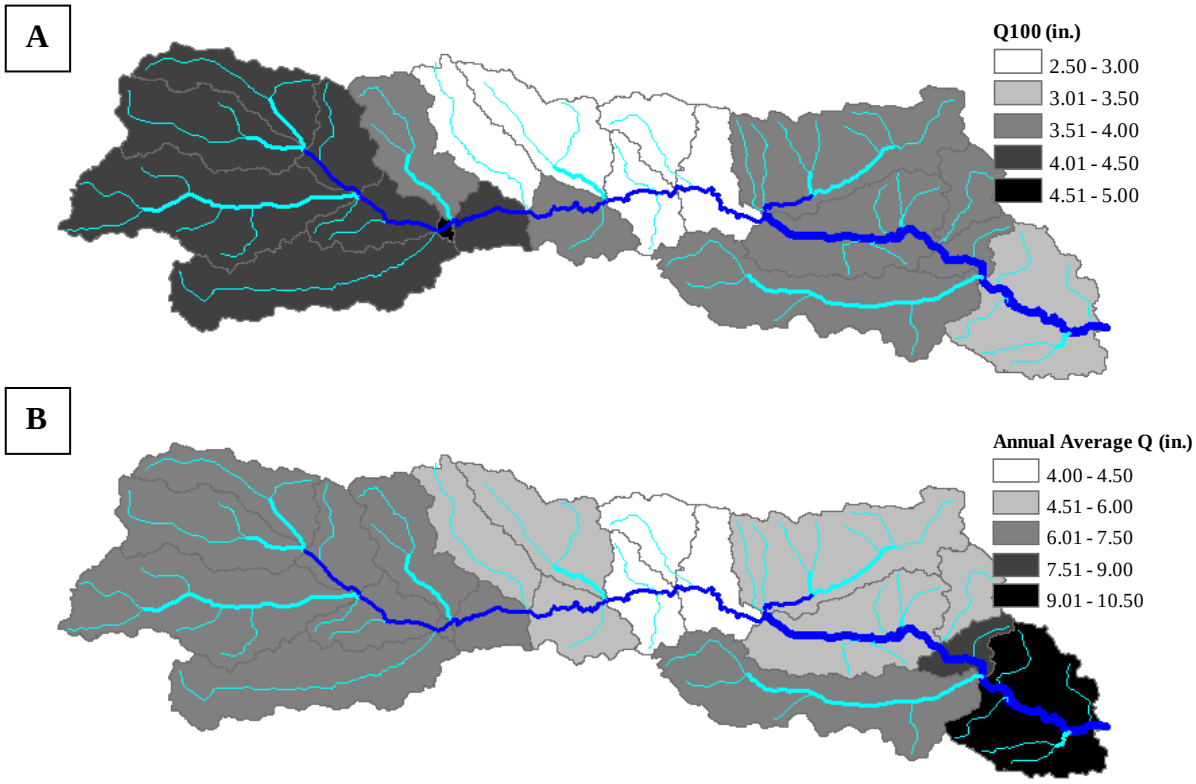

Figure 1. (A) Runoff volumes for each sub-watershed in Clear Creek for the 100-yr, 24-hour event. (B) Annual average runoff for each sub-watershed in Clear Creek.

The WEPP/ event simulations were conducted for six measured rainfall events, along with design storms ranging from the 2-yr, 24-hr event to the 100-yr, 24-hr event for a representative

hillslope in Clear Creek. Using variable initial conditions, approximately 180 simulations were run producing an average runoff depth of 2.875 cm and sediment concentration of 13.125 g/l. These values were used to help set the experimental conditions for some laboratory studies of the Alternative Tile Intakes. These laboratory studies will be used to determine trapping efficiencies that can be as inputs for modeling of these BMPs.

4) Summary and Conclusions

Progress during this year was limited due to the transfer of the PI and one of the co-PIs from the University of Iowa to the University of Tennessee. The grant has been frozen for this transfer since August of 2013. Currently the project transfer is nearing completion, so that progress will continue.

5) Listing of publications that have resulted from this research

Dermisis, D., A.N. Papanicolaou, B. Abban, and D. Flanagan. Dynamic approach for predicting soil transport and delivery from fields and small catchments to headwater streams: field experiments and analysis. Earth Surface Processes and Landforms. In Preparation (2014).

Papanicolaou, A.N., M. Elhakeem, C.G. Wilson, C.L. Burras, L.T. West, B. Clark, and B. Oneal. Understanding the variability of saturated hydraulic conductivity at the hillslope scale due to soil property heterogeneity induced by land management and erosion. Hydrological Sciences Journal. In Preparation (2014).

6) Student support provided by this research

The following students received at least partial support (both funded and unfunded) from this project: Ben Abban, Will Ettema

7) Achievements and awards for this research

n/a

8) Any additional funding this research has received

The information gathered from this project was used to develop the following proposals:

Understanding TBCA processes in intense agricultural landscape: an improved vertical and horizontal representation of SOC and litter movement across the landscape and deciphering of the contributions of root, litter, and soil decomposition to TBCA.
National Aeronautics and Space Association – U.S. Department of Agriculture - U.S. Department of Energy – National Oceanic and Atmospheric Administration: Carbon Cycle Science
09/14 - 09/16
$550,000
PI: A.N. Papanicolaou
Declined

CNH: Interactions among changing climate, agricultural markets, and bioenergy: Implications for environmental quality, farm production structure, and rural well-being.
08/13 - 07/16
$1,500,000
National Science Foundation – Dynamics of Coupled Natural Human Systems
PI: A.N. Papanicolaou
Declined

Increasing the Resilience of Agricultural Production in the Tennessee River Basin through More Efficient and Less Impactful Use of Water Resources.
10/14 - 09/19
$5,000,000
U.S. Department of Agriculture, Agriculture and Food Research Initiative.
PI: F. Walker (A.N. Papanicolaou, Co-PI)
Pending

The Effect of Smart Farm Technology on Sustainable Agroecosystems.
10/14 - 09/19
$5,000,000
U.S. Department of Agriculture, Agriculture and Food Research Initiative
PI: D. Bennett (A.N. Papanicolaou, Co-PI)
Declined

Award--Hysteresis in Index-Velocity Rating Curves

Basic Information

Title:	Award--Hysteresis in Index-Velocity Rating Curves
Project Number:	2013IA246S
Start Date:	1/1/2013
End Date:	8/31/2013
Funding Source:	Supplemental
Congressional District:	
Research Category:	Climate and Hydrologic Processes
Focus Category:	Hydrology, Surface Water, Methods
Descriptors:	
Principal Investigators:	Richard Cruse, Marian V.I. Muste, Marian V.I. Muste

Publication

1. Lee, Kyutae. "Evaluation of methodologies for continuous discharge monitoring in unsteady open-channel flows." PhD diss.,University of Iowa, 2013.http://ir.uiowa.edu/etd/5012.

Grant G13AP0008

U. S. Army Corps of Engineers
Chicago District,
Chicago, Illinois

HYSTERESIS
IN INDEX-VELOCITY RATING CURVES

Grant Report

Principal Investigators

Marian Muste

Kyutae Lee

IIHR-Hydroscience & Engineering

The University of Iowa

Iowa City, December 30, 2013

Summary

The accuracy of discharge estimation in Chicago Sanitary and Ship Canal (CSSC) has been extensively investigated through numerous studies to ensure that the withdrawal rates and volumes from Lake Michigan are in compliance with the Supreme Court Decree stipulated in 1967. Despite the vast amount of effort spent for substantiating the discharge estimation accuracy, these efforts still continue as the flow and measurement environment in CSSC pose considerable challenges. Among them are the validity and accuracy of the rating curves during the propagation of unsteady flows through the CSSC system.

Ratings curves are conventional means to continuously provide estimates of discharges in rivers. Among the most-often adopted assumptions in building these curves are the steady and uniform flow conditions for the open-channel flow that in turn provide a one-to-one relationships between the variables involved in discharge estimation. The steady flow assumption is not applicable during propagation of storm-generated waves and other time-varying perturbations hence the question on the validity and accuracy of the steady rating curves during unsteady flow are of both scientific and practical interest.

The present study focuses on the impact of temporal flow variations in CSSC on the accuracy of index-velocity rating curve (I-VRC) in use at Lemont gaging station. Unsteady flows propagating at this station result from the superposition of multiple perturbations (unsteady pulses) occurring in the system both upstream and downstream the gaging station. Currently, the literature does not offer comprehensive criteria for evaluation of the methods for estimation of the departure of the looped rating curves from the steady ones nor for identifying the most appropriate means to dynamically capturing hysteresis for different flow conditions.

Despite the limited amount of data available for analysis, the main conclusion of the study is that the I-VRC used at the Lemont gaging station perfoms better than the widely-used stage-discharge rating curve. This superiority is well demonstrated though analytical and numerical evidence garnered in CSSC as well as by observations drawn from prior studies. Data analysis of the direct discharge measurements used to construct the I-VRC at Lemont gaging station, time series for main variables associated with selected storm events, along with the implementation of analytical methods for substantiating the hysteresis lead to the findings of practical significance.

The positive nature of findings resulted from this study confirms that the protocols for tracking the flow in the system are appropriate. However, the present study is based on a limited dataset that precluded thorough and definite assessment of the accuracy of the I-VRC discharge estimation during all types of transient flows that might occur in the system. Consequently, the study ends by recommending a set of tasks for further consideration that can better substantiate the accuracy of the rating curves during steady and unsteady flows. It is expected that these additional studies will provide the foundation for a framework that can be extended to other gaging stations based on index-velocity measurement approaches (e.g., acoustic, image-based or radars). The developed framework can be readily applied to real-time streamgage networks for enhancing exploration in river science and support decision making of practical aspects related to rivers processes.

Table of content

Summary 2

1. Introduction 8
   1.1. Background 8
   1.2. Considerations on discharge estimation in CSSC 10

2. Study overview 13
   2.1. Approach and objectives 13
   2.2. Methods and Tasks 15
   2.3. Constraints 15

3. Illustration of I-VRC Performance in Prior Case Studies 17
   3.1. General Considerations 17
   3.2. Experimental Evidence 17

4. Hysteresis in CSSC (from here on the figs and tables need to be renumbered) 22
   4.1. Introduction 22
   4.2. Analysis of the Calibration Data for the Lemont Gaging Station 23
   4.3. Types of Flow Events in CSSC 26
      4.3.1. Drawdowns 30
      4.3.2. Drawdowns combined with large storm events 37
   4.4. Analytical Investigation of Hysteresis in CSSC 41
   4.5. Additional Considerations on I-VRCs 44
   4.6. Discussions and findings 47

5. Conclusions and recommendations 49

References 51

List of Figures

Figure 1 Example of hysteresis in the stage-discharge rating curves for a variety of river sizes: a) small stream (Gunawan, 2010); b) medium stream (Faye and Cherry, 1980); c) and d) large rivers (Fread, 1975, Herschy, 2009, respectively). Source: Lee (2013). 9

Figure 2 Layout of the Chicago Sanitary and Ship Canal and tributaries (Espey et al., 2009)..... 11

Figure 3 Definition sketch for terms used in the discussion 14

Figure 4 Flood event in Ebro River: (a) storm hydrograph; (b) cross section at the gaging site and depth-averaged velocity distribution for one of the transect (stage 5.3m)..... 18

Figure 5 Unsteady flow effects on: (a) the h-QRC; (b) the time sequence of the discharge, mean velocity, and depth variation during the event 20

Figure 6 Analysis results for I-VRC: succession of the velocity profiles on: a) the ascending limb; (b) the descending limb; (c) relationship between channel stage and depth average velocity derived from ADCP direct measurements; d) the index velocity profiles corresponding to two quasi equal flow depth on the rising and falling limbs (circles on the plot displayed in Figure 6 (c); e) comparison between steady RC, Fread correction method, h-QRC obtained using the I-VRC protocol, and direct ADCP measurements..... 21

Figure 7 Direct discharge measurements used for calibration of the I-VRC at the Lemont gaging station (Jackson et al. (2012): a) the I-VRC using calibration data acquired between 2004-2011; b) calibration points plotted in the stage-discharge coordinates. 24

Figure 8 Flow events associated with the "outlier" direct discharge measurements plotted in Figure 7: a) storm inflow (9/15/2008); b) quasi-steady-flow (6/3/2010); drawdown flow (10/24/2011)..... 25

Figure 9 Location of the rain gages in the Chicago River basin. The analysis uses Gage 6, 10, and 10 located in the centroids of Chicago River basin, the study area for the LMDA, and the Calumet River basin, respectively (Espey et al., 2009). 27

Figure 10 General layout of the Lockport controlling structures (Straub et al. 2012). The inset displays the schematic of the 7 sluice gates comprising the Lockport Controlling Works (LCW).28

Figure 11 Detailed view of the Lockport Power House (PH) controlling structures (Straub et a. 2012). The figure details Area 2 in Figure 10..... 29

Figure 12 The November 22-24, 2010 storm as described by precipitation, control structure sequencing, and streamflow recorded at the Lemont gaging station a) stage and discharge time series; b) stage-discharge relationship; c) time series of discharge and precipitation; d) time

history of precipitation, stage, and timing of the operation at the Lockport controlling structures 33

Figure 13 The July 18-20, 2012 storm (Event 1 in Table 3) as described by precipitation, control structure sequencing, and streamflow recorded at the Lemont gaging station: a) stage and discharge time series; b) stage-discharge relationship; c) time series of discharge and precipitation; d) time history of precipitation, stage, and timing of the operation at the Lockport controlling structures..... 34

Figure 14 The July 24, 2012 storm (Event 3 in Table 3) as described by precipitation, control structure sequencing, and streamflow recorded at the Lemont gaging station: a) stage and discharge time series; b) stage-discharge relationship; c) time series of discharge and precipitation; d) time history of precipitation, stage, and timing of the operation at the Lockport controlling structures..... 35

Figure 15 The August 4-5, 2012 storm (Event 4 in Table 3) as described by precipitation, control structure sequencing, and streamflow recorded at the Lemont gaging station: a) stage and discharge time series; b) stage-discharge relationship; c) time series of discharge and precipitation; d) time history of precipitation, stage, and timing of the operation at the Lockport controlling structures..... 36

Figure 16 Comparison of the h-QRC surrogate with I-VRC discharge estimates: a) h-QRC obtained using the available direct discharge measurements during drawdowns; b) comparison of discharge time series obtained with the two alternative RCs..... 37

Figure 17 The July 22-26, 2010 storm event (Events 1 and 2 in Table 3) as described by precipitation, control structure sequencing, and streamflow recorded at the Lemont gaging station: a) stage and discharge time series; b) stage-discharge relationship; c) time series of discharge and precipitation; d) time history of precipitation, stage, and timing of the operation at the Lockport controlling structures 39

Figure 18 The August 26-28, 2012 storm (Event 2 in Table 3) as described by precipitation, control structure sequencing, and streamflow recorded at the Lemont gaging station: a) stage and discharge time series; b) stage-discharge relationship; c) time series of discharge and precipitation; d) time history of precipitation, stage, and timing of the operation at the Lockport controlling structures..... 40

Figure 19 Streamwise profiles and cross sections for the main stem of the CSSC system (Source: Charles Shatuk Hill, 1986) 42

Figure 20 Comparison between discharges estimated with I-VRC at Lemont and Fread's method for S_o=0.00005 and n=0.023 43

Figure 21 Experimental evidence illustrating hysteresis in I-VRC: a, b) laboratory studies by Graf & Qu (2004) and Tu et al. (1995), respectively; c) field data by Nihei & Sakai (2006) 45

Figure 22 Influence of the H-ADCP location for I-VRC at the Lemont gaging station: a) typical vertical velocity distribution laws for various ranges of velocities (Jackson et al. (2012); b) influence on the I-VRC with the change in the vertical location of the H-ADCP. 46

List of Tables

Table 1 The original research tasks 16

Table 2 Time stamps and discharges recorded for the outliers in Figure 7. 23

Table 3 Events considered in Jackson et al., 2013 study 26

Table 4 Timing of the operations at the Lockport controlling structures for the November 22-24, 2010 storm 31

Table 5 Timing of the operations at the Lockport controlling structures for the July 18-20, 2012 storm (Event 1 in Table 3) 31

Table 6 Timing of the operations at the Lockport controlling structures for the July 24, 2012 storm (Event 3 in Table 3) 32

Table 7 Timing of the operations at the Lockport controlling structures for the August 4-5, 2012 storm (Event 4 in Table 3) 32

Table 8 Timing of the operations at the Lockport controlling structures for the July 22-26, 2010 storm event (Events 1 and 2 in Table 3) 38

Table 9 Timing of the operatiosn at the Lockport controlling structures for the August 26-28, 2012 storm (Event 2 in Table 3) 38

Table 10 Power law used in conjunction with the AVM for estimating the depth-averaged velocity at Lemont gaging station 45

1. Introduction

1.1. Background

The acquisition of continuous river discharge measurements is critical for hydrologic and hydraulic applications as well as for many water-related domains (e.g., environmental, social, and economic) as they all require knowledge of the river past, current and future stream flows. Given its importance, the continuous and real-time estimation and communication of the discharge is a desirable asset for a wide range of monitoring, forecasting and planning authorities. Producing a discharge record assumes direct measurement of velocities and depths over the entire stream cross-section. Given the time and financial effort involved to directly measure discharges (especially during high flows), recursion is made to an indirect approach where discharge estimation is based on Rating Curves (RC).

RCs are constructed over time with directly measured discharges by repeating several times over the year to cover the range of flow occurring in the stream and obtain significant data samples for building the RCs. Direct discharge measurements combined with analytical methods and engineering judgment provides persistent relationships among flow governing variables. After RC establishment, one or more variables are continuously measured typically in real time hence they can be used in conjunction with the RCs to provide continuous estimation of the discharge. The variables selected to be continuously measured are typically easier to measure. The continuously-measured variables are the stream stage, the velocity in one point or across the stream cross section, or the free surface slope determined from two instruments deployed at a given distance along the stream. The most popular method to provide continuous estimation of discharges is the extensively used stage-discharge RC that ingests direct stage measurements. There are many places and situations where estimation of discharges based on RCs is an acceptable surrogate instead of the more expensive direct discharge measurements. The discharge estimates are provided in many cases near-real time, with frequencies of the order of tens of minutes.

There are three main protocols for continuous discharge estimation: stage-discharge, index-velocity, and slope-area methods (Rantz et al., 1982). Given that complexity and variety of the flow situations that can occur in natural conditions, RCs are typically constructed using simplifying assumptions. Among the most-often adopted assumptions are the steady (unchanging in time) and uniform (streamlines do not change along the river reach) flow conditions. For these simple flow conditions, the RCs are represented by one-to-one relationships between the variables involved in streamflow estimation. More specifically, RCs at any point in time are characterized by a unique set of dynamic variables (depth, velocity, and discharge). While these unique relationships are not valid for unsteady flows, the steady RCs are extensively used for both steady and unsteady flows under the widely adopted judgment that they are sufficiently accurate for practical purposes irrespective of the nature of the flow unsteadiness.

The departure of the unsteady limbs from the one-to-one relationships is generically labeled "loop" (Henderson, 1966) or hysteresis (defined in general terms as the dependence of a system not only of the present state but also of its past). The magnitude of the departure of the non-unique relationships from the one-to-one relationships is site and event specific and reflects the degree of flow unsteadiness. There is experimental evidence that indicate that the differences between the discharges estimated with steady state-discharge RCs and actual discharges propagating during unsteady flows can be relatively large in comparison with, for example, the uncertainty associated with the direct discharge measurements. The latter uncertainty is considered acceptable for values less than 5%. Figure 1 illustrates results of direct measurements acquired during propagation of unsteady flows in four widely different stream sizes. These differences range between 15 and 41 % for discharge (at the same stage) and between 10 and 26% for stage (at the same discharge). Lindner and Miller (2012) found 20-30% difference between the discharges on the rising and falling limb of the hydrographs even in less than 1 m deep in-channel urban streams.

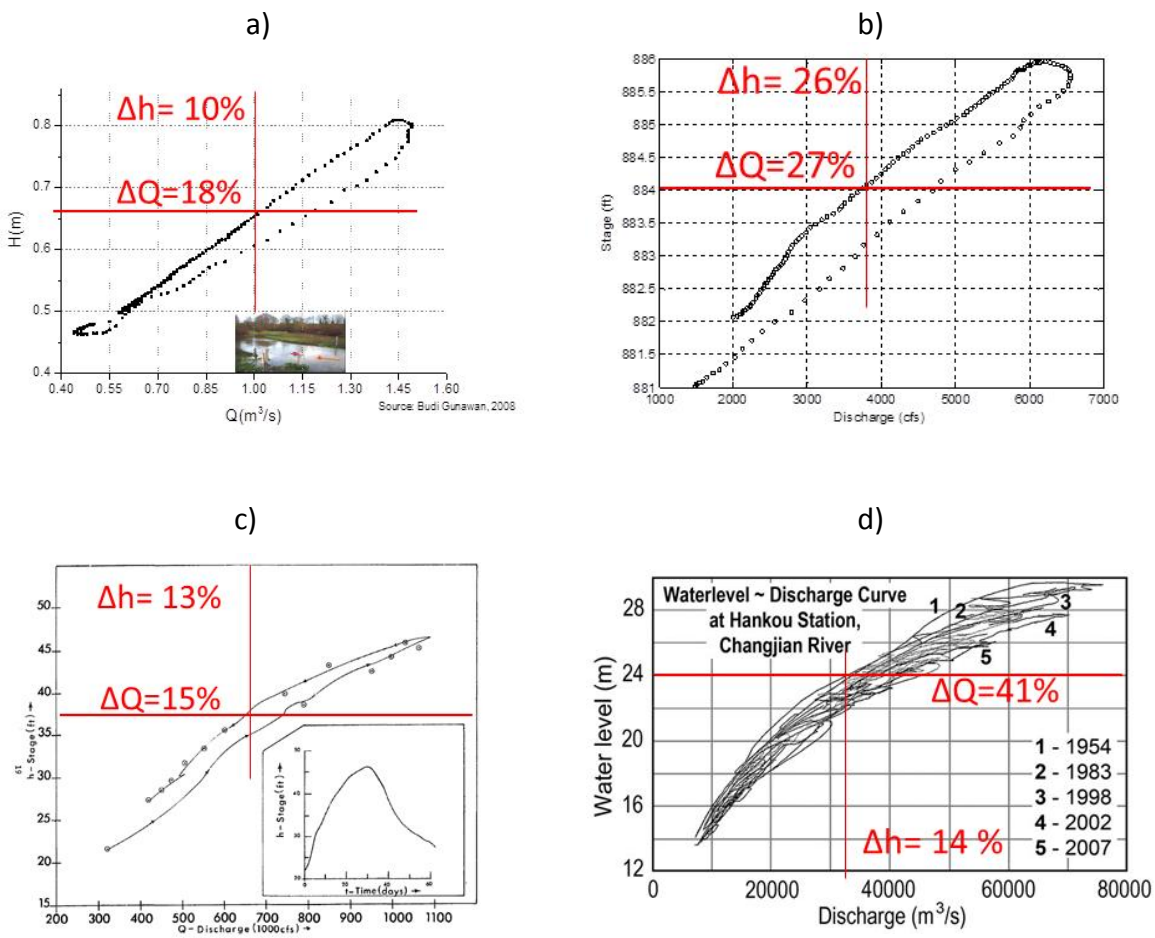

Figure 1 Example of hysteresis in the stage-discharge rating curves for a variety of river sizes: a) small stream (Gunawan, 2010); b) medium stream (Faye and Cherry, 1980); c) and d) large rivers (Fread, 1975, Herschy, 2009, respectively). Source: Lee (2013).

As can be observed in the plots illustrated in Figure 1, the main impact of the unsteady flows on the RCs built under steady flow assumptions consists in the fact that the dependencies between variables are not anymore unique for all the phases of the flow propagation. These non-unique dependencies established have been illustrated both for stage-discharge RCs (Henderson, 1966; Schmidt, 2002) and for index-velocity RCs (Ruhl and Simpson, 2005; Nihei and Sakai, 2006; Nihei and Kimizu, 2008). The non-uniqueness of the RCs stems from the different rates of the acceleration (on the rising limb) and deceleration (on the falling limb) associated with the propagation of flood hydrograph.

When relying on steady RCs for estimating discharges in unsteady flow situations, the departure of the actual discharges from the RCs is analogous to an uncertainty that persist as long as the storm wave propagate through the gaging station. The most reliable method to capture this departure is the direct acquisition of discharge measurements during the whole duration of the unsteady event. With the advent of the new generation of acoustic instruments these measurements are increasingly possible as illustrated by agencies such as USGS in the U.S. that are programmatically targeting flood events for strengthening the data sample used for building RCs. Hysteresis has only received interest in flood-prone large rivers (e.g., Mississippi) with the purpose to better understand the process and provide more accurate data for the streamflow forecasting models (National Weather Service, personal communication).

In the last decades however, medium and small rivers such as Iowa and Cedar Rivers in Iowa, experienced floods with an increased frequency. For this smaller size rivers there are no systematic efforts to evaluate the impact of hysteresis on the accuracy of the RC used in flood prediction and monitoring. These situations require an event-based monitoring to capture the dynamic of the flow propagation. However, these more complex and costly measurements are rarely done as there is a perception in the hydrometry community that the hysteresis effects on RCs are small and cannot be discerned from the uncertainty of the instruments and methods used to build the RCs. Consequently, many unsteady events on small and medium inland rivers go by undocumented. The acquisition of such experimental evidence can uniquely support the sound evaluation of effect of hysteresis on current monitoring practices and eventually lead to optimized algorithms for improved quality of the RCs for all river sizes.

1.2. Considerations on discharge estimation in CSSC

The objectives of the present study are to complement prior and on-going research on the accuracy and reliability of the USGS discharge measurements and the methods to compute discharge continuously in Chicago Sanitary and Ship Canal (CSSC) system. The CSSC system illustrated in Figure 2, is under intense and continuous scrutiny since the construction of the system at the beginning of the 20th century when the Chicago River flow was reversed allowing to send diluted wastewater effluent downstream to the Mississippi River and away from the city's freshwater source. A U.S. Supreme Court decree limits the diversion from Lake Michigan to an annual mean discharge of 3,200 cfs. Implementation of this decree requires an accurate computation of the discharge and assessment of the uncertainty in discharge data. The annual withdrawal budget is obtained using a combination of analytical, measurements, and numerical tools assembled in the Lake Michigan Diversion Accounting (LMDA) protocol. LMDA is described

in the report of the sixth technical review committee (Espey et al., 2009). The present study focuses on the significance and uncertainty assessment induced by unsteady flow events (hysteresis) into the index-velocity protocols for continuously estimating the discharge at the USGS gaging station near Lemont (IL). This station is a key component to the LMDA.

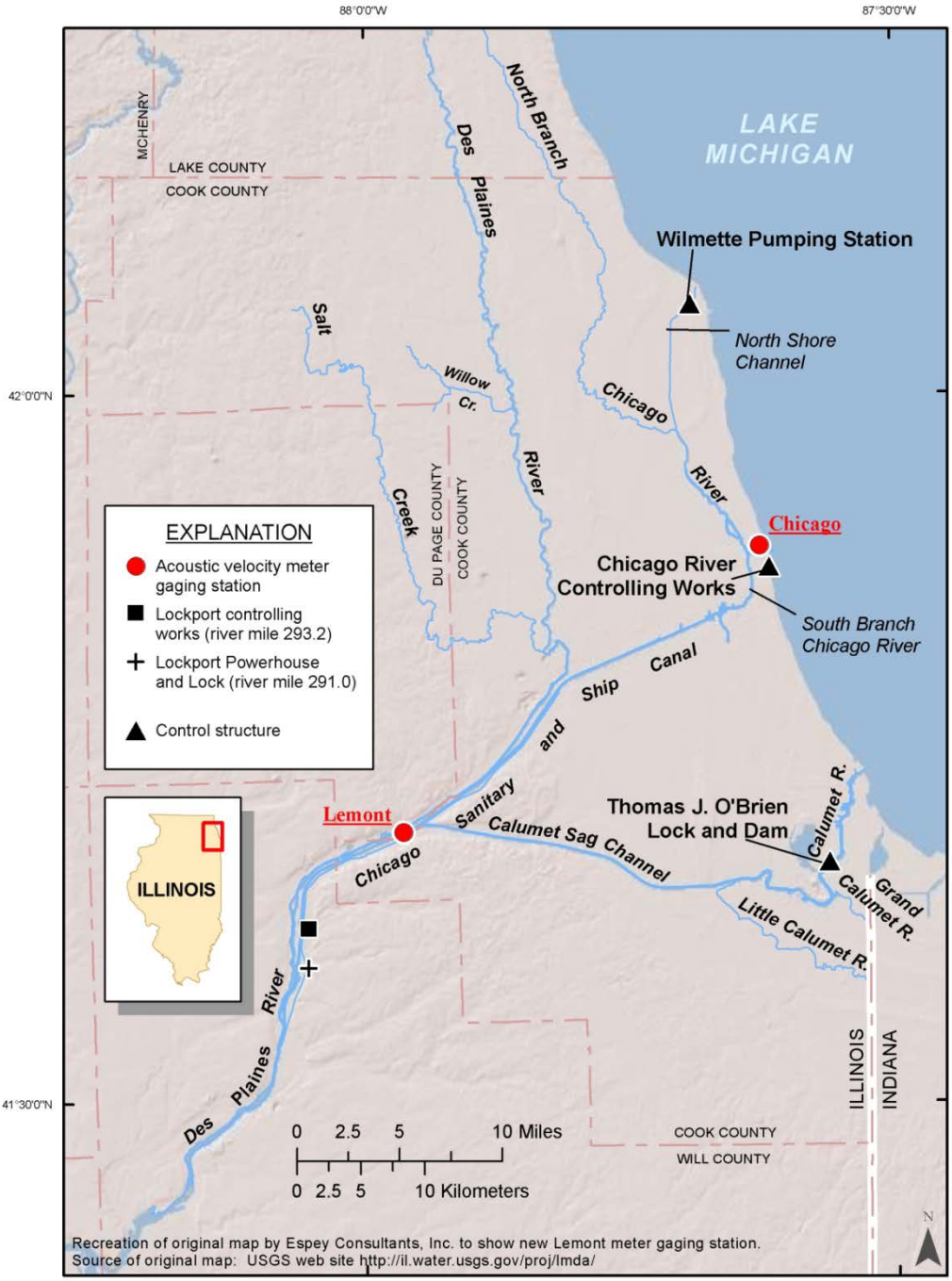

Figure 2 Layout of the Chicago Sanitary and Ship Canal and tributaries (Espey et al., 2009)

Lemont gaging station operates continuously since 2004 using a three-path Accusonic ORE 7510 GS acoustic velocity meter (AVM), a Teledyne RD Instruments Channel Master acoustic Doppler velocity meter (H-ADCP), a ParaScientific pressure sensor (PS-2), a staff gage and ancillary recording and communication components (Jackson, et al., 2012). Following the suggestions of the sixth technical review committee (Espey et al., 2009), a subsequent study established the suitability of replacing the AVMs with the H-ADCP as a primary index velocity meter to be included in the estimation of withdrawal from Lake Michigan (Jackson et al., 2012). A related problem that was raised by the technical committee is the impact of the unsteady flows in CSSC on the construction and use of index-velocity rating curves (I-VRC). The follow up study conducted by USGS (Jackson et al., 2012) documented the existence of flow unsteadiness in CSSC system. Jackson et al. (2012) identified 9 different dominant frequencies caused by flow unsteadiness in the system. Customized measurements and numerical simulations have been initiated to document the findings.

The preliminary conclusions of the Jackson et al. (2012) study are: a) temporal averaging is necessary to remove the influence of hysteresis in the I-VRC, b) secondary flows appears to be responsible for large difference between the rated and measured discharge at low discharges, c) the H-ADCP is a suitable replacement for the AVM as index velocity meter near Lemont gaging station (despite adversities of flow characteristics and geometry of the gaging site). The study acknowledges that the examination of the vertical and transverse velocity profiles for a range of flows and temporal averaging periods revealed that although the instantaneous vertical velocity profiles may be highly variable, the time-averaged profiles are generally consistent with the open-channel theory. Throughout the observations, calibration, and analysis of I-VRC conducted in the above-mentioned study, it was assumed that the flow in the channel is steady.

Another subsequent and related study focused on CSSC was published in 2013 with special consideration of the impacts of the flow non-uniformity and flow unsteadiness on the accuracy of the index-velocity based RC at Lemont (Jackson et al., 2013). This new study investigates whether the hysteresis can occur in CSSC and under which conditions using both a theoretical approach and a three-dimensional hydrodynamic model. The theoretical approach tackles the hysteresis produced by the non-uniform spatial distribution of the flow in the Lemont gaging station. This analysis is extremely valuable as it brings to light an additional complexity of the rating curves that has been rarely investigated in the literature (actually these authors are not aware of similar prior studies). The three-dimensional model was used to assemble index-velocity RCs for the Lemont station by sampling the simulation results with virtual instruments placed in the numerical domain according with the geometry of the real instruments used to acquire the index velocity and the mean flow across the section. The study found that none of the six simulated flow events produced substantial hysteresis and that they agreed relatively well with the experimental measurements used to construct the index-velocity RC at Lemont.

The overall conclusions of the two distinct investigative approaches used in the Jackson et al (2013) study led to the conclusion that there is no conclusive evidence for existence of hysteresis in the index-velocity RCs at the Lemont station. Although the theoretical analysis

indicates the possibility of hysteresis occurrence at this site, the hydrodynamic conditions required to generate hysteresis are not present at this site based on historical data.

2. Study overview

2.1. Approach and objectives

The previous section provided general information on steady RCs and their performance in unsteady flows as well as the conclusions of prior studies that tackled the subject of hysteresis in CSSC. Jackson et al. (2013) study on the potential of hysteresis development mentioned in Section 1.2 is the first such study in CSSC and among the few existing ones dealing with the hysteresis in index-velocity RCs. The only publications that mention, but not actually substantiate, evidence of hysteresis in inland streams are the USGS reports describing the protocols for establishing index-velocity RCs: Morlock et al (2002) and Levesque and Oberg (2012). Another relevant report is Ruhl and Simpson (2005) study with focus on the construction of RCs for gaging stations in tidal areas.

The present study complements the CSSC studies mentioned in Section 1.2 by approaching the hysteresis analysis from a perspective similar to the extensive literature on hysteresis in stage-discharge RCs. Such studies are, for example, those conducted by Schmidt (2002) and Petersen-Overleir (2006). These studies investigate hysteresis with practical approaches based on the one-dimensional flood routing equations (Henderson 1966). Typically these relationships link general flow conditions to a "normal" steady condition on the steady stage-discharge RC. Normal flow often refers to average, or typical flow conditions (Schmidt, 2002). The generic relationships between the discharge Q for any condition and the "normal" discharge Q_n is provided by Knight (2006) as shown in the equation below (see also Figure 3):

$$Q = \underbrace{\left(A\sqrt{R}\right)K\sqrt{S_0}}_{Q_n}\sqrt{\underbrace{1}_{a} - \underbrace{\frac{1}{S_0}\frac{\partial h}{\partial x}}_{b} - \underbrace{\frac{U}{gS_0}\frac{\partial U}{\partial x} - \frac{1}{gS_0}\frac{\partial U}{\partial t}}_{c}} \qquad (1)$$

where A is the flow cross section area; U is the mean flow velocity in the cross section; R is the hydraulic radius; K is a conveyance coefficient (which can be obtained from Chezy, Darcy-Weissbach, or Manning); S_0 is the bed slope; h is the flow depth; and x is the distance in streamwise direction.

Discarding the last three terms of the equation, leaves us with the steady normal flow equation assumed for the construction of the steady RCs. Consideration of more than the first term in equation (1) provides a more realistic description of the flood routing (i.e., non-uniform, unsteady flow) that results in changes of the shape and position or loops in the curves. Specifically, the equation's terms indicate different types of flood routing model: kinematic wave (term *a* only), diffusion wave (terms *a* and *b*), and full dynamic wave (terms *a*, *b*, and *c*).

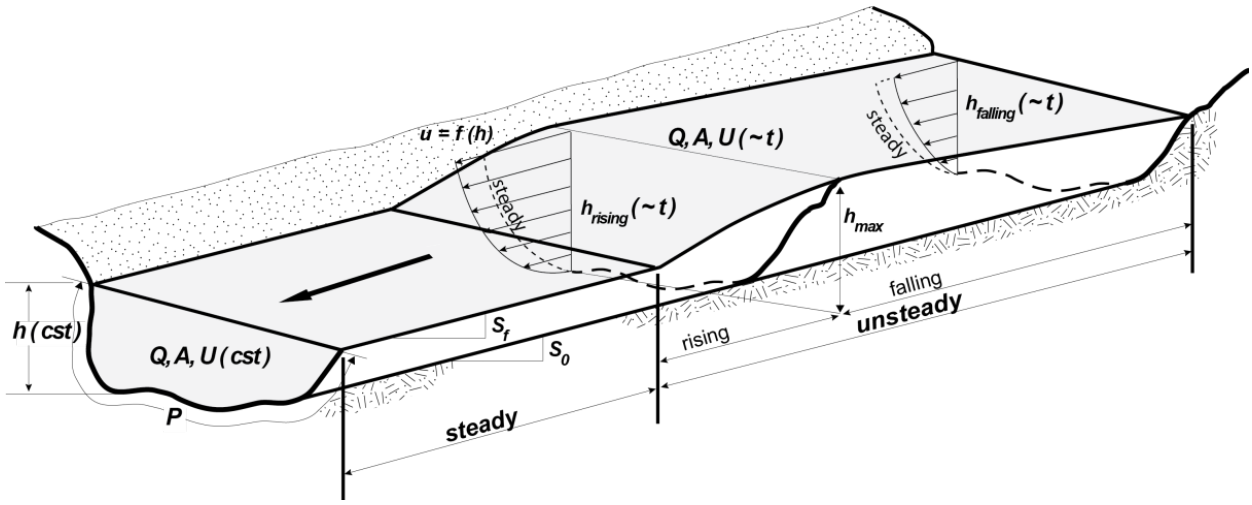

Figure 3 Definition sketch for terms used in the discussion

The assumption associated with the present analysis is that the flows maintain their streamline uniformity in steady and unsteady flow. This hypothesis is adequate if the channel geometry (cross section) is not changing considerably along the waterway as it is the case for the CSSC man-made canal. In the absence of flow spatial non-uniformity it can be assumed that there are no backwater effects that would further complicate the analysis of hysteresis. Another assumption of the analysis is that the Manning's roughness coefficient does not change during the flow propagation. This is also an acceptable statement for CSSC system whereby the canals were dug in limestone for the majority of their length. Consequently, the present investigative approach attributes any departure of the discharges from the steady rating curves to unsteadiness of the flow.

The unsteady channel flow situations occur during transient events such as the surges produced by the inflow of runoff excess associated with rainfall events. Urban streams offer particular challenges from this respect as the surges in the streams are generated by short-duration high-intensity summer thunderstorms occurring on largely impervious areas. In these situations, it is often difficult or impossible to collect direct discharge measurements at high flows both because of dangerous conditions in the channel and also because the stream rises and falls so rapidly that field crews cannot reach sites in time and sometimes cannot make measurements rapidly enough to keep pace with changing water levels even when they are on site during a storm (Lindner and Miller, 2012). These practical obstacles preclude the acquisition of the experimental evidence so much needed to validate various aspects of hysteresis in RC.

The objectives of this study are to:

a) investigate the impact of hysteresis on the index-velocity based rating curves (I-VRC)
b) assess the significance of the hysteresis in I-VRCs for CSSC system conditions
c) propose a measurement and data reduction protocol that accounts for the hysteresis effect using the instrumentation available at the Lemont gaging station (if the effect is found significant)

2.2. Methods and Tasks

Similarly to backwater- and overbank flow-induced uncertainties, the hysteretic effect does not affect RCs before and after the flood-wave passing as they are active just while the storm event unfolds. Consequently, a random direct discharge measurements protocol (sampling the flow at various times during steady and unsteady flows) as currently used in operations is not deemed appropriate for documenting unsteady flows as it will mix the characteristic of the flow during rising and falling phases leading to one-to-one relationship for the RC. The present study attempts to employ an event-based, unsteady flow approach to determine the significance of the hysteresis in I-VRCs and assess the impact of neglecting it in routine operations. We adopt the event-based approach as the hysteresis-induced effect is only present when the flow is unsteady (i.e., during flood wave propagation) therefore the need to continuously and frequently sample the flow during the duration of flow unsteadiness.

Such analysis potentially leads to two mean velocity ratings for the same channel: one corresponding to the rising phase, and another one for the falling stage of the hydrograph. The proposed approach is similar to the segmented approach proposed by Ruhl and Simpson (2005) for constructing index-velocity RCs for tidal areas (see the description on this subject in Appendix C of the report). This more complex data acquisition and processing protocol is required to properly capture the hysteretic nature of the I-VRCs. The only conceptual difference between the flow in tidal areas and the one during the propagation of a storm (flood) wave in a channel is that the unsteady flow is periodical for the former and non-periodical for the latter process.

The overall intent of this study is not aimed at replacing the current I-VRCs protocols rather to assess the uncertainty interval associated with the use or steady RCs during unsteady events. The initial plan for the study was to investigate the I-VRCs using measured data and/or results of numerical simulations conducted in previous studies for Lemont station by Jackson et al. (2012) and Jackson et al. (2013) if the datasets are collected or simulated over time scales commensurate with the lifetime the unsteady events. It was proposed to analyze the existing data and simulation results using data mining and analytical tools based on the governing equations for unsteady channel flows. By doing so, the results of the present study can be aligned with previous results reported in the literature dealing with hysteresis. The original tasks of the investigation are provided in Table 1.

2.3. Constraints

During early stages of the study, the research team found that there are no direct ADCP measurements acquired continuously during the storm events and sampled with a frequency commensurate with the lifetime of the unsteady flows occurring in the CSSC system. It was hoped that the set of results of numerical simulations can be used as surrogate for the input data needed in the proposed analysis. For this purpose, our research team requested the project manager to arrange a meeting with the research team that developed the numerical simulations in order to assess if the simulation results can support with relevant data the

present investigation. During the meeting between the two research teams, results of the simulations reported in Jackson et al. (2013) were thoroughly discussed.

The discussions revealed that the flow arriving at the Lemont station during unsteady flows is the result of the combination of:

- flow pulses (equivalent to unsteady flows) generated by runoff arriving in the system at different times in the CSSC and Cal-Sag channels
- flow perturbations produced by maneuvering the Lockport powerhouse and/or controlling works in order to produce drawdowns in CSSC.

The time difference between the flow pulses in CSSC and Cal-Sag channels is proportional to the storm intensity and channel lengths upstream of the confluence of the two channels. The flow perturbations at Lockport powerhouse are decided by the Metropolitan Water Reclamation District of Greater Chicago (MWRDGC) personnel when considerable storms are forecasted. The superposition of all these simultaneous flow pulses generated in various points of the system leads to a complex superposition of unsteady flow propagating through the Lemont station. A description of the flow superposition is provided later in the report.

Table 1 The original research tasks

T.1	**Data mine unsteady flow events documented by concurrent direct H-ADCP and ADCP measurements in CSSC (full-cycle data, i.e., drawdown followed by the flood wave from major unsteady events are needed for the analysis)**
T.2	**Data mine unsteady flow events documented by the 1-D (Espey et al., 2009) and the recent 3-D numerical simulations provided by Jackson et al. (2013). The diagnostic for T.1 and T.2 will be guided by the dominant frequencies and corresponding time periods (from 16 to 350 minutes) identified in CSSC at Lemont by Jackson et al. (2012) study.**
T.3	**Use the records identified at T.1 and T.2 to analyze the changes of the shape of the velocity profiles for rising and falling stages of the events (several verticals across the channels will be analyzed to capture both the generality of the trends as well as to verify the unsteadiness effect on the transverse velocity distribution)**
T.4	**Reconstruct the index-velocity RC using direct measurements and results of numerical simulations commensurate with the timeline of the event. Vertical profiles will be analyzed progressing in time as the event unfolds, rather than lumping them irrespective of the unsteady phase (rising or falling) in subgroups based on the velocity magnitude (as previously analyzed in Jackson et al., 2012).**
T.5	**Analyze the stage-area and index velocity-mean velocity relationships for the events identified at T.4 for the effect of hysteresis. Extend the analysis for other events that are documented through direct high temporal resolution measurements to substantiate the analysis.**
T.6	**Estimate the differences between the discharges obtained using the protocol based on steady rating curve and the analysis conducted in Task T.5 for each event and compare the differences across events.**
T.7	**Using the protocols described in T.4 to T.6, evaluate the effect of using steady versus unsteady I-VRC on longer term discharge records to assess the significance of different protocols for LDMA objectives**
T.8	**If the differences at T.7 are significant (differences of more than ±5%), develop measurement and analysis protocol that account for the presence of unsteady flows in CSSC and provide associated recommendations.**

The complex superposition of unsteady pulses propagating at the Lemont station cannot be solved with the analytical methods originally planned for the study, i.e., the 1D flood propagation and correction methods such as those developed by Jones (1916) or Fread (1975). These methods are usable for uniform flows subjected to single flow pulse (unsteadiness) whereby they substantiate well the significance and the uncertainty associated with hysteresis. Next section demonstrates such case studies to illustrate the typical hysteresis analysis method implementation. This analysis can be implemented in the CSSC conditions only for situations when just one source of unsteadiness is propagating through the gaging station. Based on the discussions with the USGS personnel that manage the Lemont station, it was found that these situations are rare, if present at all in the CSSC system. This situation does not rule out the development of hysteretic behavior in the CSSC, rather explain that the tools to analyze its significance are not available and their development is beyond the scope of the present study. It is hypothesized herein that the combination of various sources of unsteadiness are diminishing the overall impact of hysteresis at Lemont station as the pulses tend to be out of phase (due to their different time of generation) and propagating in opposite directions (the runoff propagates downstream, the drawdowns propagate upstream). This hypothesis requires further analysis and customized experiments.

3. Illustration of I-VRC Performance in Prior Case Studies

3.1. General Considerations

Currently, there are instruments, legacy data, and analytical approaches that can improve our understanding of the significance of hysteresis for small and large rivers and that can facilitate the development of appropriate protocols for the assessment of hysteresis in a systematic manner (Muste and Lee, 2013). Our discussion on hysteresis is limited herein to simple flow situations with the intent to quantify the unsteadiness-related hysteresis effect in isolation from other potential effects on RCs. Specifically, we analyze the effect of flood flow propagation in channels controlled by friction (channel control) rather than local controls where backwater is inherently involved (Sassi et al., 2011). Furthermore, the hysteresis-related uncertainty is estimated only for in-bank flow situations as the change in cross section occurring during floodplain flows generate additional uncertainties that are difficult to separate from the mix. This section presents evidence of the hysteretic behavior in stage-discharge and index-velocity RCs and the non-unique connection between variables based on a data acquired in the field with adequate instruments and event-based sampling measurement protocols. This section replicates approximately verbatim a previous study on the subject (Muste and Lee, 2013) to illustrate the benefits and assessments that are relevant for the present study.

3.2. Experimental Evidence

The advent of the hydroacoustic instruments, especially ADCPs, has made possible the development of discharge-measurement systems capable of more accurately measuring flows affected by unsteadiness. An ADCP-based discharge-measurement system is dramatically faster

than conventional ones and has comparable or better accuracy. ADCP experiments require, however, a significant amount of operator training on the flow and acoustic physics as well as knowledge of ADCP operation, software, and ancillary techniques involved in the measurement process. The need for these special skills added to the fact that storm events are rare and still pose measurement challenge makes it difficult to obtain reliable sample data for understanding and substantiating the importance of unsteady rating curves in practical situations.

One of the few sets of such data was collected at a gaging station located in the Ebro River by Ferrer et al. (2013). The station provides continuously discharges using stage measurements acquired by a float-counterweight system that are subsequently fed in the h-QRC established for the station. The gaging station is located about 100 km upstream from its sea mouth and downstream from a series of dams for flood control. Given the controls available in the system, unsteady flows can be created through dam operations for various purposes. Two such "artificial" floods were captured using high-density stage-discharge data uniformly spread over the duration of the hydrograph passing (18 data pairs for the first events and 28 for the second). Figure 4(a) replicates the hydrograph for the second (approximately half day) event along with the 28 direct stage-discharge measurement pairs taken at about 30 minutes interval. Discharge measurements were acquired by two teams using Sontek M9 ADCPs (http://www.sontek.com/riversurveyor-s5-m9.php). The stream cross section at the gaging location and the range of depth (stage) variation during the flood propagation are shown in Figure 4(b). Figure 4(b) also illustrates a selected depth-averaged distribution in the channel indicating that the flow is relatively uniform.

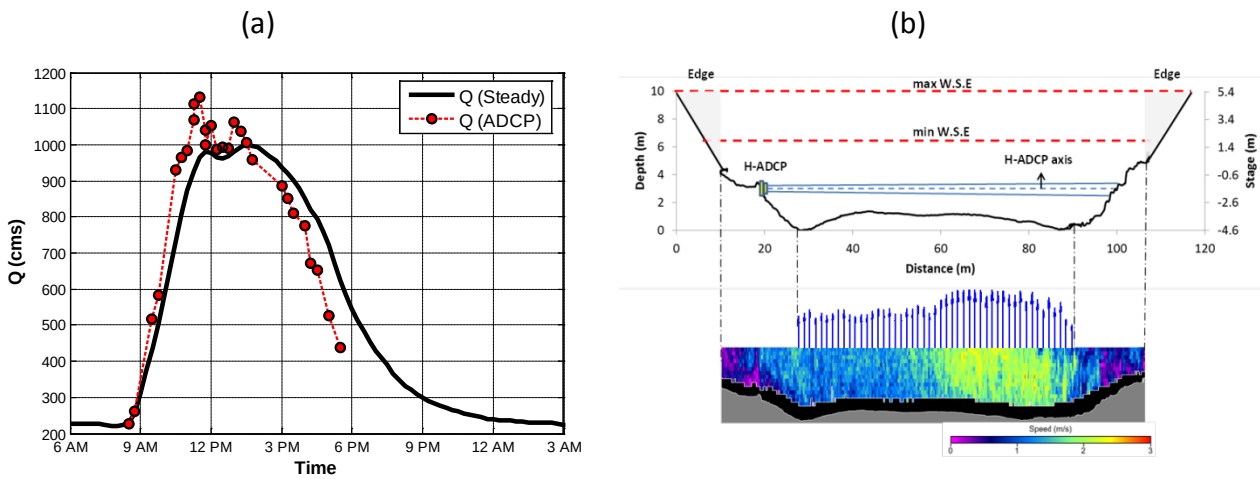

Figure 4 Flood event in Ebro River: (a) storm hydrograph; (b) cross section at the gaging site and depth-averaged velocity distribution for one of the transect (stage 5.3m)

Figure 5 illustrates the impact of the flood wave propagation through the gaging station on the h-QRC. Figure 5(a) show the steady h-QRC used at the time of measurements and the looped RC formed by the ADCP measured discharges. Also plotted in the figure is the looped RC

obtained with Fread's analytical correction formula applied to the steady RC (Fread, 1975). This method is based on the full one-dimensional unsteady channel flow equation. It can compute either stage or discharge once the temporal variation (time derivative) of the other variable is given. Stage or discharge can be provided by either observations or estimations. Fread (1975) made the following assumptions for deriving his method.

- Lateral flow is negligible.
- The width of a channel is constant along the stream.
- Energy losses due to friction and turbulence are described by Manning's equation.
- The geometry of cross-section is assumed constant (no sediment deposition or erosion)
- The bulk flood wave moves downstream as a kinematic wave (water surface slope approximately equals to the bottom slope).
- The flow at the cross-section is controlled by the channel geometry, friction, bottom slope, and the type of flood waves.

By using the full one-dimensional unsteady channel flow equation, Manning's equation, and the space derivative introduced by Henderson (1966) (equation (2), the final form of Fread method (1975) is shown in equation (3).

$$\frac{\partial y}{\partial x} = -\frac{1}{c}\frac{\partial h}{\partial t} - \frac{2S_0}{3r^2} \tag{2}$$

$$Q - 1.486\frac{AD^{2/3}}{n}\left[S_0 + \left[\frac{A}{KQ} + (1-\frac{1}{K})\frac{BQ}{gA^2}\right]\partial h_S + \left(\frac{\frac{Q'}{A'} - \frac{Q}{A}}{g\Delta t}\right) + \frac{2S_0}{3r^2}\left(1 - \frac{BQ^2}{gA^3}\right)\right]^{1/2} = 0 \tag{3}$$

where S_0 is channel bed slope; $K = \frac{5}{3} - \frac{2A}{3B^2}dB/dh$; r is the ratio of the channel bed slope to the entering wave slope; $r = \frac{56200(Q_P - Q_O)}{(h_P - h_o)\bar{A}}\tau S_0$; Δt is the computational time step, in sec; Q' is the discharge at time t-Δt, in ft^3/sec; A' is the cross-sectional area at time t-Δt, in ft^2 ; ∂h_S is the change in water surface elevation during the Δt time interval, in ft/sec; $\bar{A}$ is the wetted cross-sectional area associated with average stage (mean stage between the base and peak); and τ is the time between base and peak flow (rising time), in days. Equation (3) can be solved iteratively to determine either the rate of change of stage or discharge when either of those parameter values is known. The latter solver is typical for implementation.

Returning to Figure 5, it can be noted that the relative differences between the discharges for the same depth and of the depths for the same discharge for corresponding points on the rising and falling limbs of the hydrograph are about 40% and 30%, respectively. These differences are approximately half if we take as reference the steady RC displayed in the figure with black continuous line. The quasi-symmetric location of the steady RC with respect to the looped RC is not typical, as observations of several datasets previously analyzed by the authors indicate that the falling limb of the looped RC is closer to the steady RC then the rising limb. Figure 5(b)

shows that the maxima for the channel velocity, discharge and stage occur at different times with a time interval between U_{max} and h_{max} of about 30 mins. The experimental data points in the two plots display inherent experimental scattering especially near the hydrograph peak where the measurement environment is more challenging. A larger than normal measurement scattering was anticipated for this dataset as the 28 reported ADCP discharge measurements are obtained from only one ADCP transect. The current ADCP operational guidelines recommend acquisition of multiple transects (at least two) or acquisition over specified minimum time durations for individual transects to produce accurate discharges (e.g., USGS, 2011). However, in the context of the present measurements, operators have to choose the right balance between measurement accuracy and the need to sample fast the rapidly time-varying event.

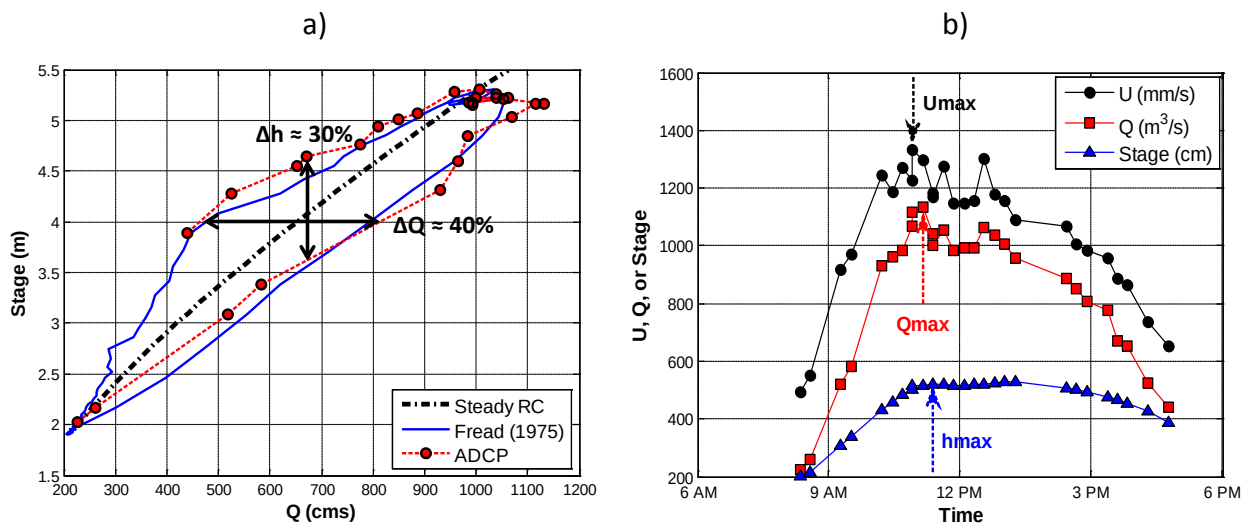

Figure 5 Unsteady flow effects on: (a) the h-QRC; (b) the time sequence of the discharge, mean velocity, and depth variation during the event

Figure 6 displays several relevant features of the I-VRC. The velocity information is provided by the direct measurements acquired with the ADCP deployed on moving boats. In order to illustrate the I-VRC method, a "virtual" H-ADCP was created herein by identifying the in-bin ADCP measured velocities along a horizontal line across the channel width. This analysis is practically equivalent to the deployment of a "virtual" H-ADCP (side-looker) that reads an index-velocity across the channel width at a given elevation as illustrated in Figure 4(b).

The analysis previously described was successively applied to 13 of the total of 28 ADCP measurements acquired during the flood event to replicate measurements of the index-velocity. Some of the measurements around the hydrograph peak were not considered in the analysis as the particular flood event show some oscillations around the peak, hence making the interpretation of these data more difficult. The width-averaged velocity at a given depth is obtained by spatially averaging the in-bin velocities identified along the line of sight (Kim et al., 2005). Application of this procedure at various depths produces a set of "virtual" H-ADCPs that provide index velocity profiles across the vertical as illustrated in Figures 6(a), 6(b), and 6(d).

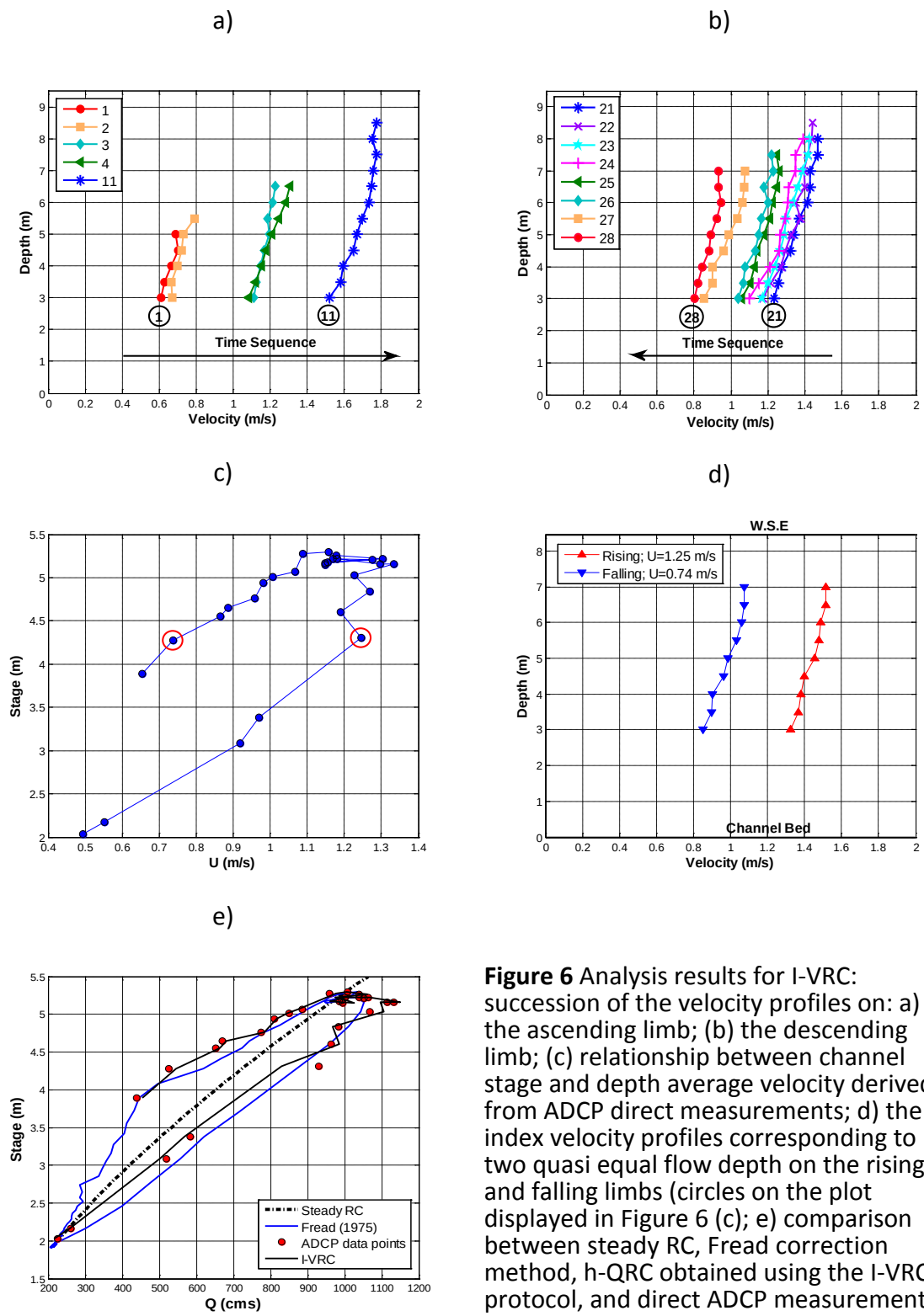

Figure 6 Analysis results for I-VRC: succession of the velocity profiles on: a) the ascending limb; (b) the descending limb; (c) relationship between channel stage and depth average velocity derived from ADCP direct measurements; d) the index velocity profiles corresponding to two quasi equal flow depth on the rising and falling limbs (circles on the plot displayed in Figure 6 (c); e) comparison between steady RC, Fread correction method, h-QRC obtained using the I-VRC protocol, and direct ADCP measurements

Selected velocity profiles acquired with the protocol described above are plotted in Figure 6(a) and 6(b). The consecutive profiles on the rising and falling limbs of the hydrograph show a continuous change of the magnitude of the velocities as well as of the flow depth. Slight differences can be noted in the shape of the velocity profiles as the flood wave propagates through the test section. Figure 6(c) visualizes the effect of flow unsteadiness on the relationship between stage and channel velocity (obtained from individual ADCP transects). Figure 6(d) displays the width-averaged velocity profiles for two direct ADCP measurements (measurement #5 and #27, red circles in Figure 6(c) acquired on the rising and falling limbs at practically the same stage (about 4.3m). Despite the slightly higher 3-D nature of Ebro River flow field, the profiles in Figure 6(d) show the same trends as those by their laboratory counterparts.

The notable aspect in Figure 6(d) is that the magnitude of the index-velocity profile is larger on the rising limb compared with the falling limb throughout the depth indicating that a "virtual" H-ADCP would read different index velocities for equal-depth points on the hydrograph limbs. Consequently, the corresponding channel velocities on the rising and falling limbs are also different. For example, the mean channel velocities corresponding to the quasi equal-depth flows identified in Figure 6(c) are 1.25 m/s and 0.74 m/s, respectively. Collectively, these combined results will lead to a looped relationship between stage and discharge relationship obtained with I-VRC method as illustrated in Figure 6(e). Specifically, the discharge used in the latter plot was established with the stage-cross section RC and the mean velocity was obtained with a one-to-one RC between the index and channel velocity. This unique relationship was obtained by following the standard protocols for index-velocity methods (e.g., Rantz et al. 1982; Levesque and Oberg, 2012; Birgand et al., 2005) for inland rivers without considering the hysteretic effects in the derivation of the I-VRC. Specifically, all the direct measurement points collected with the ADCP disregard of their event phase (rising or falling) were used to estimate the index velocity RC for the H-ADCP deployed at a stage of 1.5m (6m from the channel bottom). The agreement between the discharges derived with the unique I-VRC relationship and the direct ADCP measurements is good with slight differences that will be discussed next.

4. Hysteresis in CSSC

4.1. Introduction

The inferences on hysteresis derived from the analysis in Ebro River case study cannot lead directly to clear-cut conclusions when applied in CSSC flow conditions. While the prismatic CSSC channel geometry is well positioned for such an analysis, the temporal and spatial accelerations (flow pulses) developing in this system are complex as described in Section 2.3. Unlike normal rivers where flow takes place due to the action of gravity downslope, in the CSSC flow takes place due to differences in water surface elevation induced by the opening of gates at Lockport and Controlling Works. The celerity of the perturbation produced by the controlling structure is in most cases larger than the mean flow velocity, meaning that hydraulic transients can propagate upstream very quickly, even during a flood event (M. Garcia, personal

communication). Moreover, the CSSC bottom slope, which is very small, plays a negligible role on the dynamics of the flow. When a flood wave reaches the end of the canal there will be a reflection and this new wave will travel upstream. While in normal rivers the flow is always in one direction, the CSSC, albeit being prismatic, experiences a range of transient flow conditions which is not easy to characterize. In summary, the use of the same analytical apparatus for substantiating the hysteresis impact as the one used in Ebro River analysis lead to inferences that are more challenging to interpret and have limited direct value for guiding the measurements protocols in the system. However, the analysis has merit in by providing useful insights and further work to assist the improvements of the measurement protocols, hence is presented below.

4.2. Analysis of the Calibration Data for the Lemont Gaging Station

Since 2004, the Lemont gaging station provides discharge estimates based on an Index-Velocity RC (I-VRC) in conjunction with direct stage (acquired with a pressure sensor, PS) and velocity measurements (acquired continuously with an acoustic velocity meter, AVM and a Horizontal Acoustic Doppler Current Profiler, H-ADCP). The construction of the I-VRC requires calibration points, i.e., direct discharge measurements acquired simultaneously with the fixed instrumentation in the station (see Figure 7.a). The 97 direct discharge measurements collected between Aug 25, 2004 and Sep 14, 2012 are plotted on stage-discharge coordinate system in Figure 7.b. Similar to the analysis conducted in Section 3, we use the stage-discharge representation in the present study as this relationship is extensively analyzed in the literature and allows concluding and comparing with knowledge inferred from prior studies. The same inferences are limited for the I-VRCs as this approach was implemented only in the last three decades and does not have the same type of benchmark data.

The data plotted in Figure 7 show large scatter and distinct regions of the stage-discharge relationship. A 2nd polynomial regression equation [labeled as Poly (ADCP) in this and subsequent figures] is also plotted to substantiate the flow regimes that this dependence captures. It can be observed that for discharges up to about 12,000 cfs the discharge decreases with the stage increase. This trend is not typical for the stage-discharge relationship whereby the relationship is typically ascendant. For larger discharges the curve seems to be ascendant as expected despite of the limited number of direct measurements in this range.

A next step in the analysis of calibration points for the I-VRC is to isolate the events that produced "outliers" in the stage-discharge relationship. Inspection of the plot in Figure 7 allows identifying four types of flow events. The numerical values for these point clusters are provided in Table 2. The time series of the flow events on which these calibration

Table 2 Time stamps and discharges recorded for the outliers in Figure 7

Group	Date & Time	Direct Q (cfs)
O1	9/15/2008 11:52	15,780
O2	6/3/2010 9:51	5,050
O3	10/24/2011 6:03	6,070
	10/24/2011 6:30	7,520
	10/24/2011 7:09	8,060
	10/24/2011 7:32	8,150
O4	1/12/2005 13:20	10,910
	8/24/2007 16:19	14,680

measurements were acquired are plotted in Figure 8. The plots in Figures 8.a), 8.b) and 8.c) correspond to the red, green, and blue circles highlighted in Figure 7. Unfortunately, there are no time series data for the events circled with black line in Figure 7.

a)

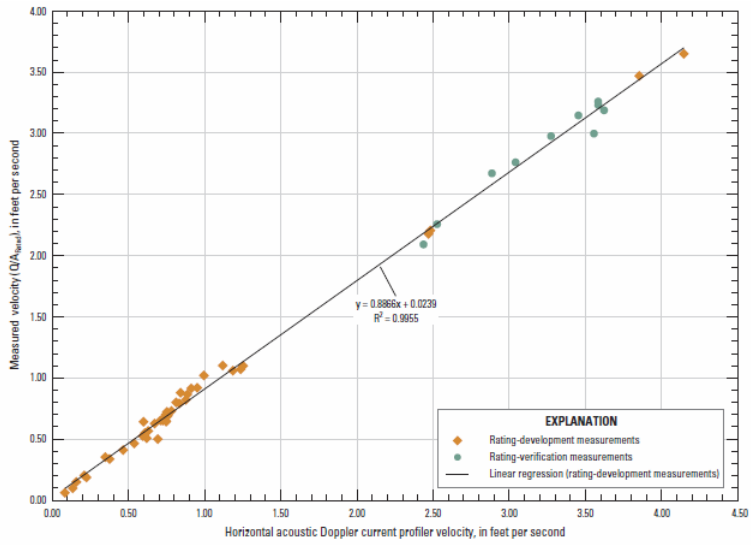

b)

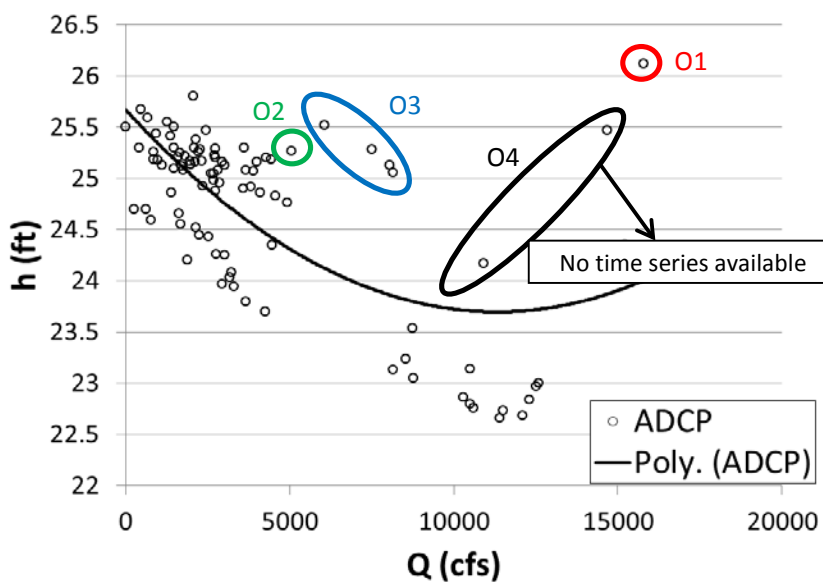

Figure 7 Direct discharge measurements used for calibration of the I-VRC at the Lemont gaging station (Jackson et al. (2012): a) the I-VRC using calibration data acquired between 2004-2011; b) calibration points plotted in the stage-discharge coordinates.

The clustering enables to identify several types of flow events that can develop in the CSSC system. The plots in figures 7 and 8 indicate that points clustered in O1 group pertain to flood-wave dominated flow (i.e., flow dominated by runoff inflows following storms in the basin); points clustered in O2 group pertain to quasi-steady-state flows (the state established in the systems in the absence of major flow perturbations), and points clustered in O3 group pertain to drawdown events. Based on the data trends, it is expected that the points clustered in the O4 group are similar to the O1 cluster. Confirmation of this hypothesis can be obtained if more calibration measurements are taken when the flow at Lemont is mostly impacted by inflow hydrographs.

An important inference related to the points in the O3 cluster: the direct discharge measurements for the four points in the cluster (see records in Table 1) were sampled about every 30 mins, therefore indicating that USGS has capabilities to accurately capture the propagation of dynamic events in the system. Such a capability is vital in documenting the impact of hysteresis on the RCs used for discharge estimation. Another inference based on the trend of the stage-discharge relationship is that most of the calibration points used to develop the I-VRC was collected during drawdowns. Consequently, the I-VRC built with these data is mostly reflective of the specific dynamics of these flow events. Based on these observations, the present study recommends that future direct measurements should include:

- Increased number of points acquired during the propagation of the inflow hydrographs produced by storms in the watershed
- Clustering of the direct discharge measurements as discussed above should be applied to all the calibration points used to support the construction and consolidation of the I-VRC in order to differentiate the dynamic vs quasi-steady state of the flow in the CSSC system and to identify the type of unsteadiness in the system (drawdowns or inflows).
- (at the extent possible) Tracking flow events continuously from drawdown to storm inflow propagation using a sampling frequency commensurate with the lifetime of the event. For example, if the storm duration is 48 hours, direct measurements should be taken at least one per hour; if the storm events is shorter, the frequency should be increased to twice per hour

a)

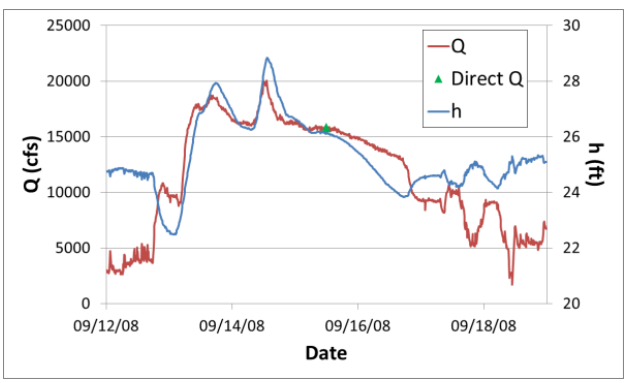

b)

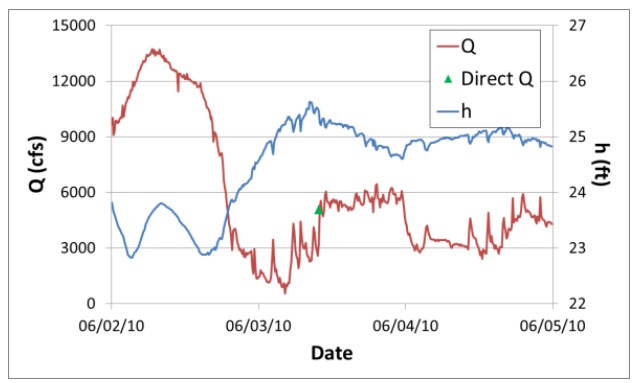

c)

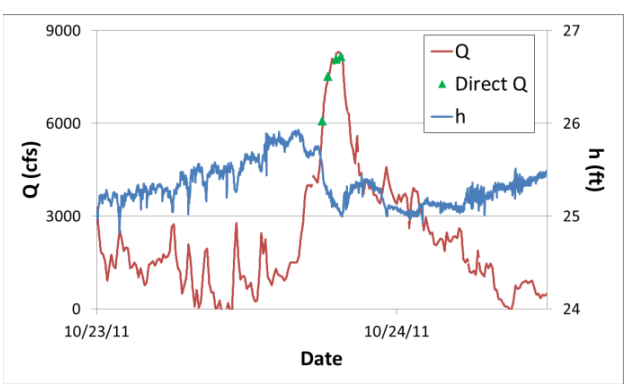

Figure 8 Flow events associated with the "outlier" direct discharge measurements plotted in Figure 7: a) storm inflow (9/15/2008); b) quasi-steady-flow (6/3/2010); drawdown flow (10/24/2011)

4.3. Types of Flow Events in CSSC

Jackson et al. (2013) have documented several flow events through the numerical simulations conducted for this study. The characteristics of the simulated events are summarized in Table 3. Typically, the events are associated with runoff inflows produced by various sizes storm events. In addition to the flow events listed in Table 3, the November 22-24, 2010 (corresponding to Figure 4 in Jackson et al., 2013) is also considered for the present analysis. For convenience and complementarity, all the above-mentioned cases will be investigated from the perspective of hysteresis impact.

Table 3 Events considered in Jackson et al., 2013 study

[CST, central standard time]

Group	Case/ Event	Duration, in hours	Start time (CST)	Peak discharge, in cubic feet per second	Synthetic flow partitioning?
Group 1	Case 1	120	00:00 July 22, 2010	18,984	Yes
	Case 2	120	00:00 July 22, 2010	18,984	Yes
Group 2	Event 1	72	12:00 July 17, 2012	12,697	No
	Event 2	102	15:00 August 24, 2012	13,366	No
	Event 3	23	22:00 July 23, 2012	8,706	No
	Event 4	33	23:00 August 3, 2012	7,237	No

In addition to the time series of velocities, stages, and discharges recorded at the Lemont gaging station, the present analysis also considers the driving factors for the flow unsteadiness, i.e., the precipitation in the watershed along with the sequence and timing of the operations executed on the control structures in the system. The precipitation data is produced by a network of raingages deployed in the Chicago River watershed as illustrated in Figure 9. The locations of the CSSC controlling structures and gaging stations using Acoustic Velocity Meters maintained by the USGS are illustrated in Figure 2. More details on the location and geometry of the Lockport controlling structures are provided in Figures 10 and 11.

Most relevant for the present analysis is the Lockport Controlling Works (LCW) and the Lockport Powerhouse (LP) operated by MWRDGC. The LCW structure consists of seven 30-feet (ft) wide sluice gates and is used to divert water from the CSSC and into the Des Plaines River (see Figure 10). The flow regimes for the sluice gate included both free and submerged weir. The LP structure consists of nine 9-ft wide by 14-ft high sluice gates and two 10-ft diameter turbines (see Figure 11). These structures have been recently rated through the USGS study, Straub et al. (2012).

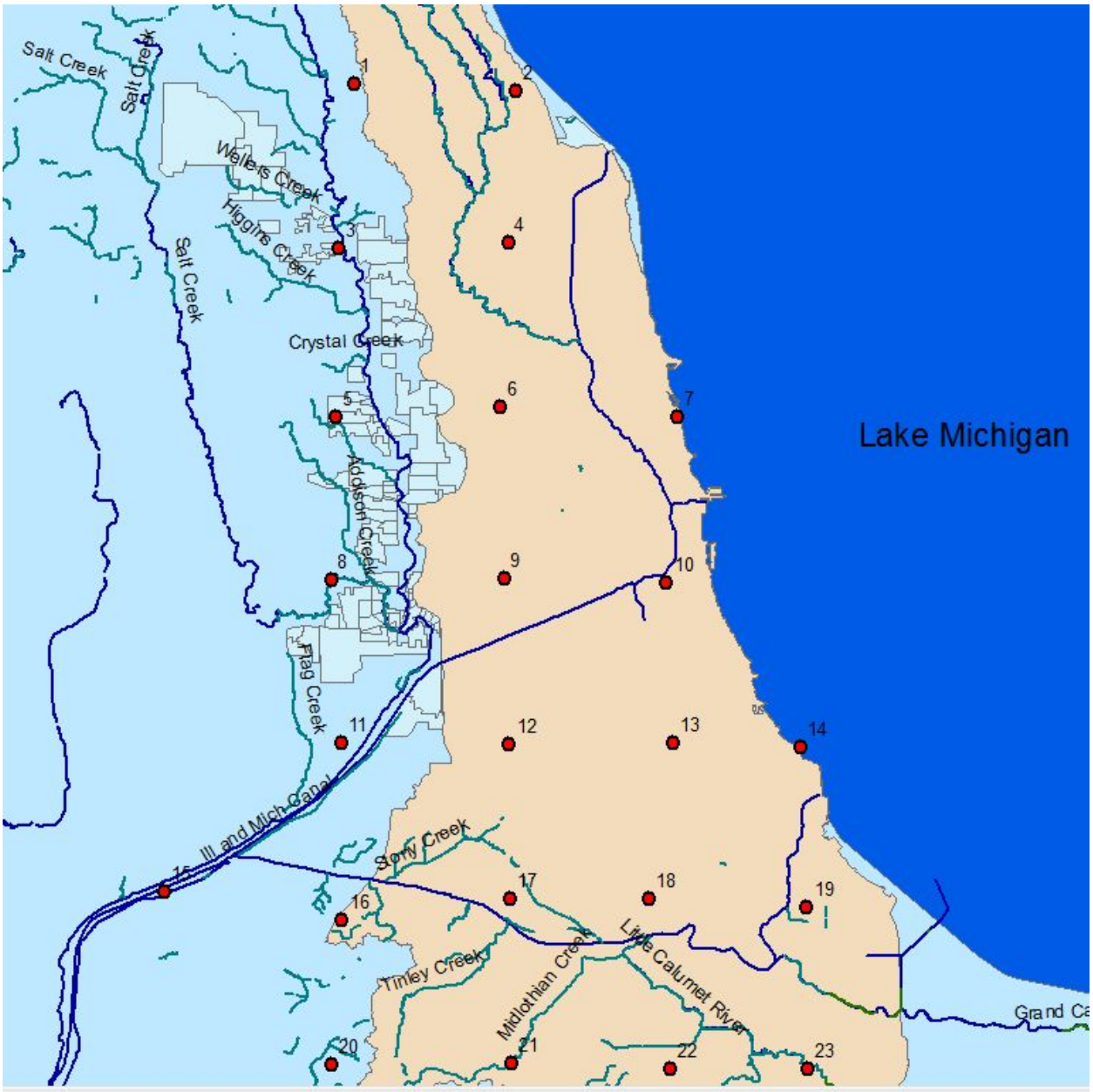

Figure 9 Location of the rain gages in the Chicago River basin. The analysis uses Gage 6, 10, and 10 located in the centroids of Chicago River basin, the study area for the LMDA, and the Calumet River basin, respectively (Espey et al., 2009).

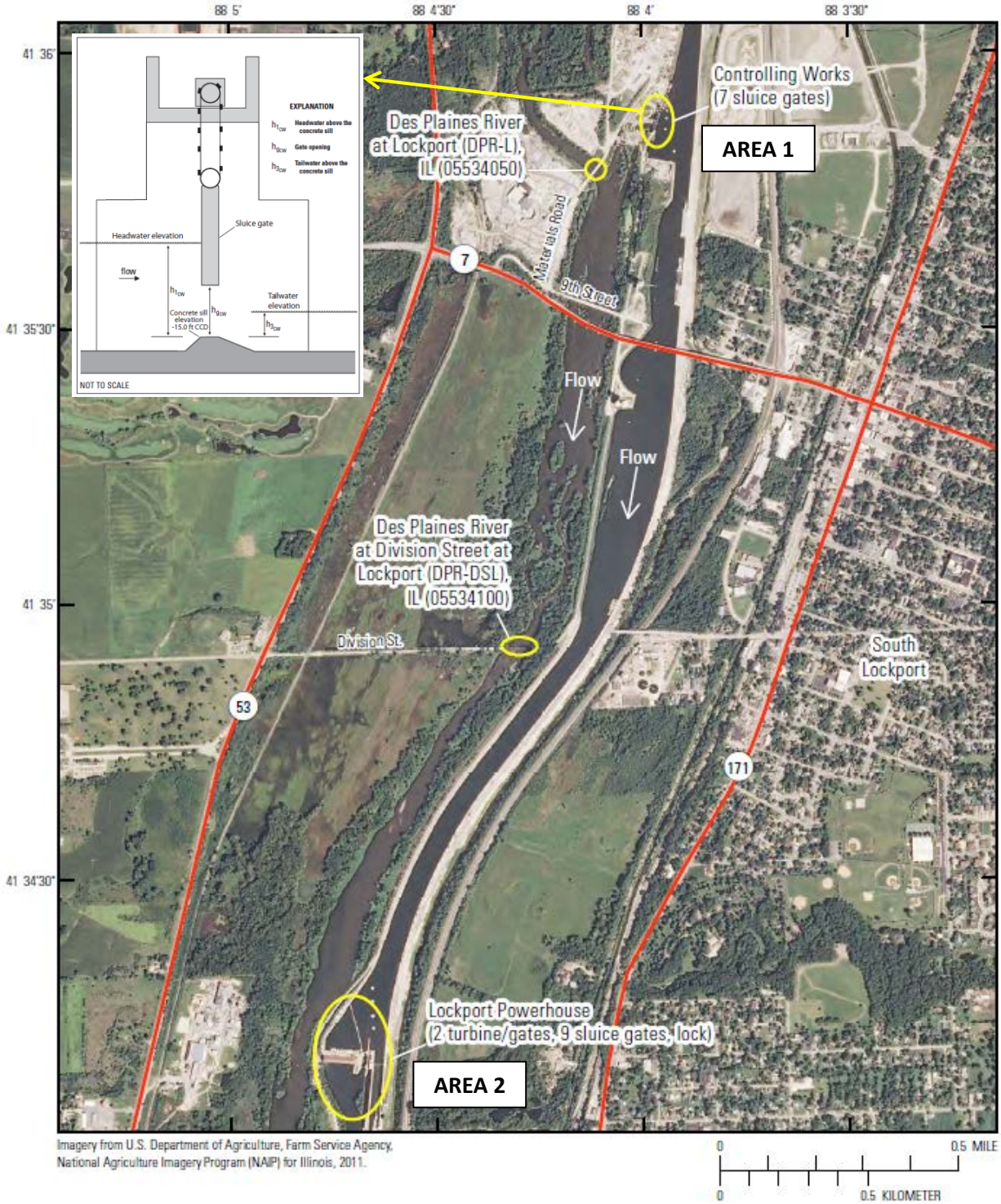

Figure 10 General layout of the Lockport controlling structures (Straub et al. 2012). The inset displays the schematic of the 7 sluice gates comprising the Lockport Controlling Works (LCW).

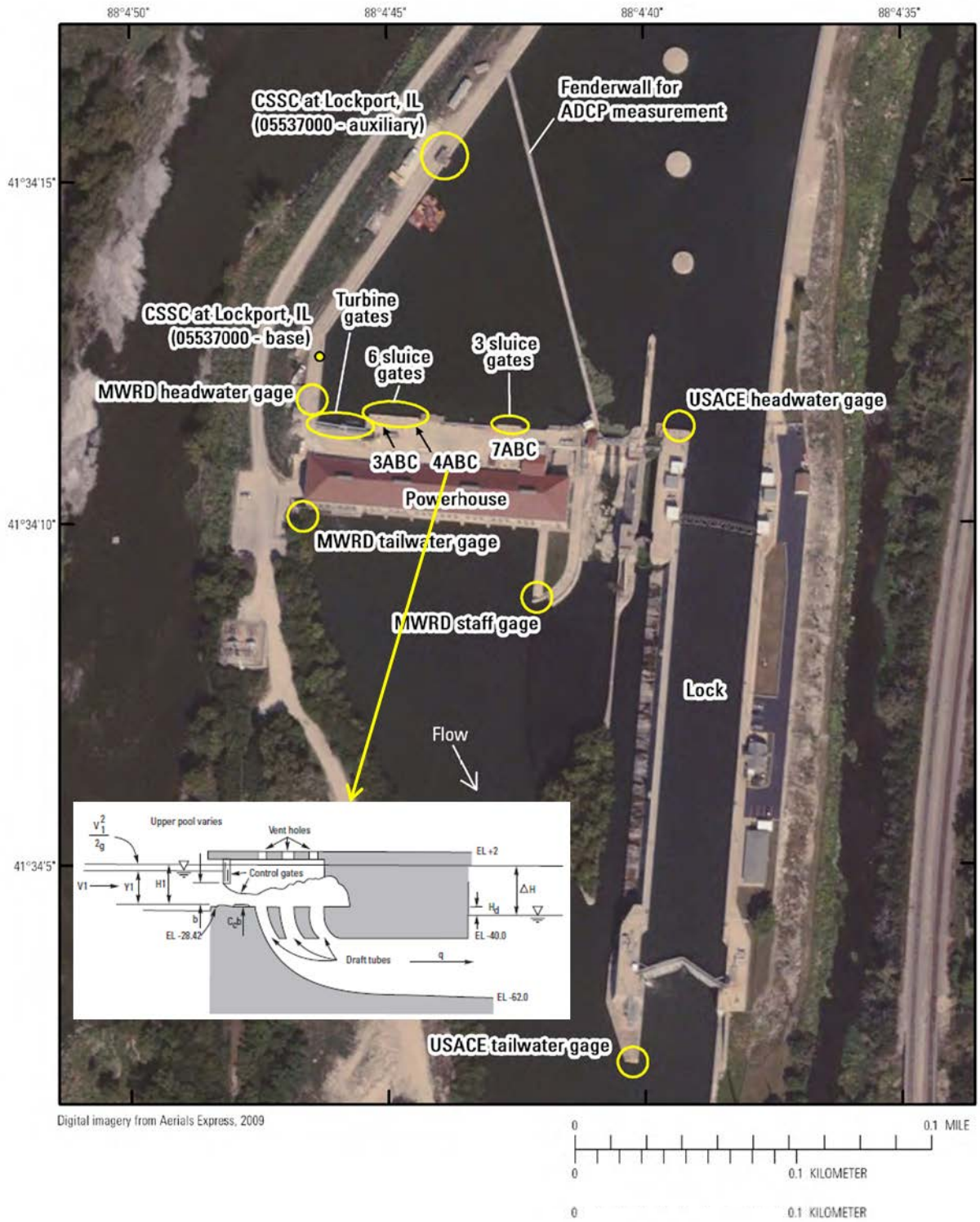

Figure 11 Detailed view of the Lockport Power House (PH) controlling structures (Straub et a. 2012). The figure details Area 2 in Figure 10.

4.3.1. Drawdowns

The first type of flow events that are analyzed herein is dominated by drawdowns triggered by the opening of the Lockport control structures (most often the Pit/sluice gates leading to the powerhouse, PH). The test scenarios from this category are labeled in Jackson et al. (2013) as November 22-24 (2010) storm event, Event 1, 3, and 4 (see Table 3). Numerical values of the metered discharges and operating sequence during the analyzed events are summarized in Tables 4, 5, 6, and 7. Figures 12, 13, 14, and 15 assemble all the relevant datasets for the events investigated by Jackson et al. (2013) in the following order: November 22-24 (2010) storm event, Event 1, Event 3, and Event 4. Each of these figures contains visualization of the stage and discharge time series for the duration of the event, the stage-discharge relationship during the event, the discharge time series along with the precipitation data, and the stage time series along with the precipitation and the timing of the operation at the Lockport controlling structures. Green upward arrows indicate gate opening while downward arrows indicate gate closing in Figures 12.d), 13.d), 14.d) and 15.d).

A common feature of the drawdown events analyzed in Figures 12, 13, 14, and 15 is that they display the same type of dependency in the stage-discharge relationship corresponding to drawdown events. The drawdown pattern is confirmed by the outlier group O3 in Figure 8.c) whereby the four sequential direct discharge measurements are unmistakable taken on a drawdown event leading to a downward h-Q relationship. During the drawdown the flow is accelerated downstream by the opening of the release gates at Lockport producing a decrease in the flow depth accompanied with an increase in discharge. This type of event is labeled herein as the “rising” limb of the hydrograph to be consistent with the conventional terminology used for describing hysteresis in rating curves. As one can observe, even as all drawdowns are associated with runoff inflows produced by precipitation, they dominate the mix of unsteady flow as indicated by the downward trend in the h-QRC. The opposite is developing when the gates are closed. Another observation revealed by Figures 12, 13, 14, and 15 is that drawdowns (typically triggered before storms) are occurring for discharges less than 12,000 cfs that might correspond to the quasi-steady state of the flow in the system.

Besides that finding that the h-Q plots of all drawdown events systematically follow a descending trend in the h-Q relationship, the plots in Figures 12, 13, 14, and 15 let one to observe that these relationships are distinct for the rising and falling stages of the hydrographs. This is consistent with the observations reported in previous studies whereby the propagation of unsteady events is associated with non-unique relationships in the h-QRC corresponding to acceleration and deceleration phases of the flow in the channel. The latter observation further indicates that unsteady cyclic events in channel flows are characterized by different vertical velocity profiles (magnitude and shape of the profile) during the rising and falling stage of the hydrographs and also different from the velocity profile for steady, uniform flows.

Table 4 Timing of the operations at the Lockport controlling structures for the November 22-24, 2010 storm

		Generators				Pit Gates			Controlling Works Gates		
Date	**Time**	**Gen#**	**Flow**	**Gen#**	**Flow**	**Pit**	**Time gate**		**CWorks**	**Time gate**	
			cfs		cfs	**Gate#**	**Opened**	**Closed**	**Gate#**	**Opened**	**Closed**
11/22/10	MID	1	1000			4B	4:34 PM	LEFT OPENED			
MON	8:45 AM	1	800	2	800	4C	5:31 PM	11:50 PM			
	9:15 AM	1	0	2	1600	7A	6:10 PM	11:30 PM		NONE	
	10:25 AM	1	0	2	1200	7B	5:55 PM	10:10 PM			
	2:30 PM	1	0	2	2000	7C	6:45 PM	10:45 PM			
	3:30 PM	1	1500	2	1500						
	4:30 PM	1	2000	2	2000						
	5:30 PM	1	2400	2	2400						
	5:50 PM	1	1200	2	1200						
	7:05 PM	1	2400	2	0						
	7:40 PM	1	1000								
11/23/10	MID	1	1000	2	0	4B	MID	12:20 AM			
TUE	2:55 AM	1	2000	2	0	7A	12:50 PM	2:40 PM			
	6:55 AM	1	1500	2	0	7B	10:20 AM	10:45 AM		NONE	
	10:45 AM	**1**	2000	**2**	2000	7B	11:20 AM	2:43 PM			
	11:43 AM	**1**	2400	**2**	0	7C	12:16 PM	2:47 PM			
	2:15 PM	**1**	1100	**2**	1100	4C	NONE				
	5:00 PM	**1**	0	**2**	0						

Table 5 Timing of the operations at the Lockport controlling structures for the July 18-20, 2012 storm (Event 1 in Table 3)

		Generators				Pit Gates			Controlling Works Gates		
Date	**Time**	**Gen#**	**Flow**	**Gen#**	**Flow**	**Pit**	**Time gate**		**CWorks**	**Time gate**	
			cfs		cfs	**Gate#**	**Opened**	**Closed**	**Gate#**	**Opened**	**Closed**
7/18/12	MID	1	1500	2	0	4A	10:35 PM	left opened			
WED	7:40 PM		2200	2	0	4B	10:00 PM	left opened		NONE	
	9:48 PM		1500	2	0	4C	8:45 PM	left opened			
	10:22 PM		2200	2	0						
7/19/12	MID	1	2200	2	0	3A	2:05 AM	11:30 AM			
THR	1:50 AM	1	1500	2	0	3B	12:45 AM	8:15 AM		NONE	
						3C	12:45 AM	1:45 PM			
						4A	MID	10:00 AM			
						4B	MID	8:00 AM			
						4C	MID	10:00 AM			
7/20/12	MID	1	1800	2	0	4B	3:10 AM	12:05 PM			
FRI	1:35 AM	1	2100	2	0					NONE	
	2:35 PM	1	1800	2	0						

Table 6 Timing of the operations at the Lockport controlling structures for the July 24, 2012 storm (Event 3 in Table 3)

		Generators				Pit Gates			Controlling Works Gates		
Date	**Time**	**Gen#**	**Flow**	**Gen#**	**Flow**	**Pit**	**Time gate**		**CWorks**	**Time gate**	
			cfs		cfs	**Gate#**	**Opened**	**Closed**	**Gate#**	**Opened**	**Closed**
7/24/12	MID	1	1500	2	0	3A	8:15 AM	9:55 AM			
TUE						3B	NONE		NONE		
						3C	6:30 AM	8:55 AM			
						4A	3:45 AM	10:45 AM			
						4B	NONE				
						4C	3:30 AM	11:30 AM			
						4C	10:50 PM	left opened			

Table 7 Timing of the operations at the Lockport controlling structures for the August 4-5, 2012 storm (Event 4 in Table 3)

		Generators				Pit Gates			Controlling Works Gates		
Date	**Time**	**Gen#**	**Flow**	**Gen#**	**Flow**	**Pit**	**Time gate**		**CWorks**	**Time gate**	
			cfs		cfs	**Gate#**	**Opened**	**Closed**	**Gate#**	**Opened**	**Closed**
8/4/12	No Generator Flows - 0					4C	MID	11:15 PM	NONE		
SAT						7C	2:05 PM	9:00 PM			
8/5/12	No Generator Flows - 0					NONE			NONE		
SUN											

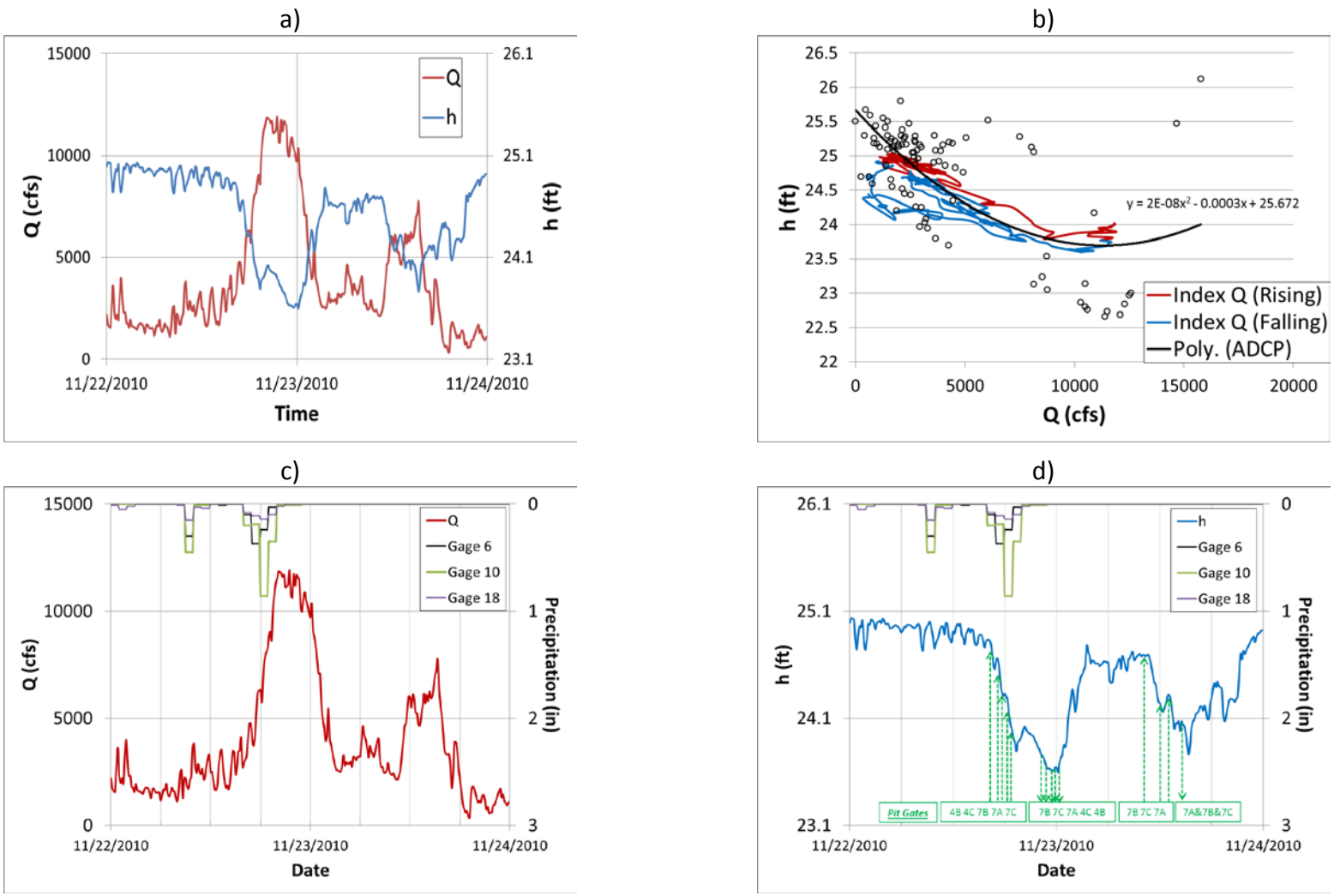

Figure 12 The November 22-24, 2010 storm as described by precipitation, control structure sequencing, and streamflow recorded at the Lemont gaging station a) stage and discharge time series; b) stage-discharge relationship; c) time series of discharge and precipitation; d) time history of precipitation, stage, and timing of the operation at the Lockport controlling structures

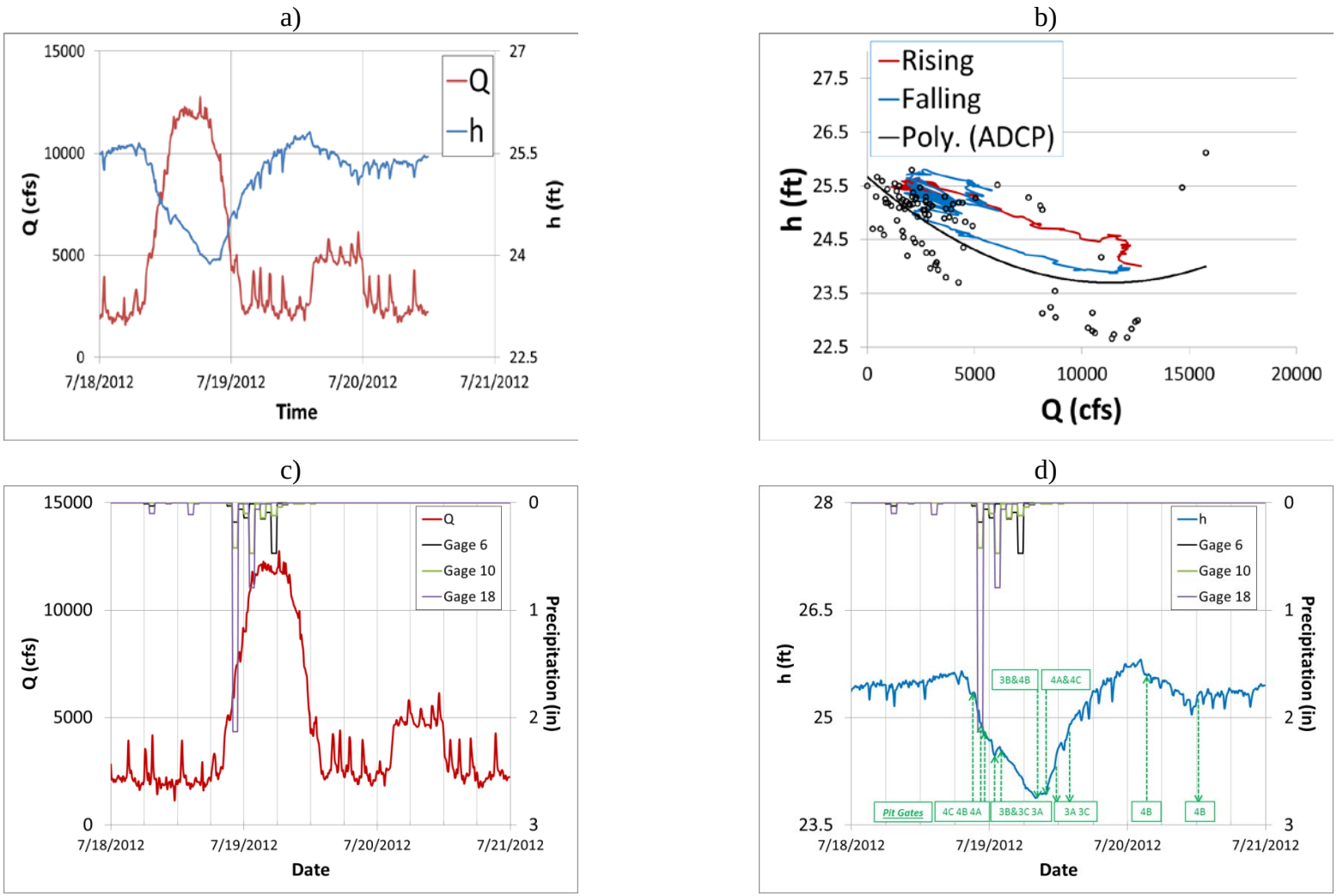

Figure 13 The July 18-20, 2012 storm (Event 1 in Table 3) as described by precipitation, control structure sequencing, and streamflow recorded at the Lemont gaging station: a) stage and discharge time series; b) stage-discharge relationship; c) time series of discharge and precipitation; d) time history of precipitation, stage, and timing of the operation at the Lockport controlling structures

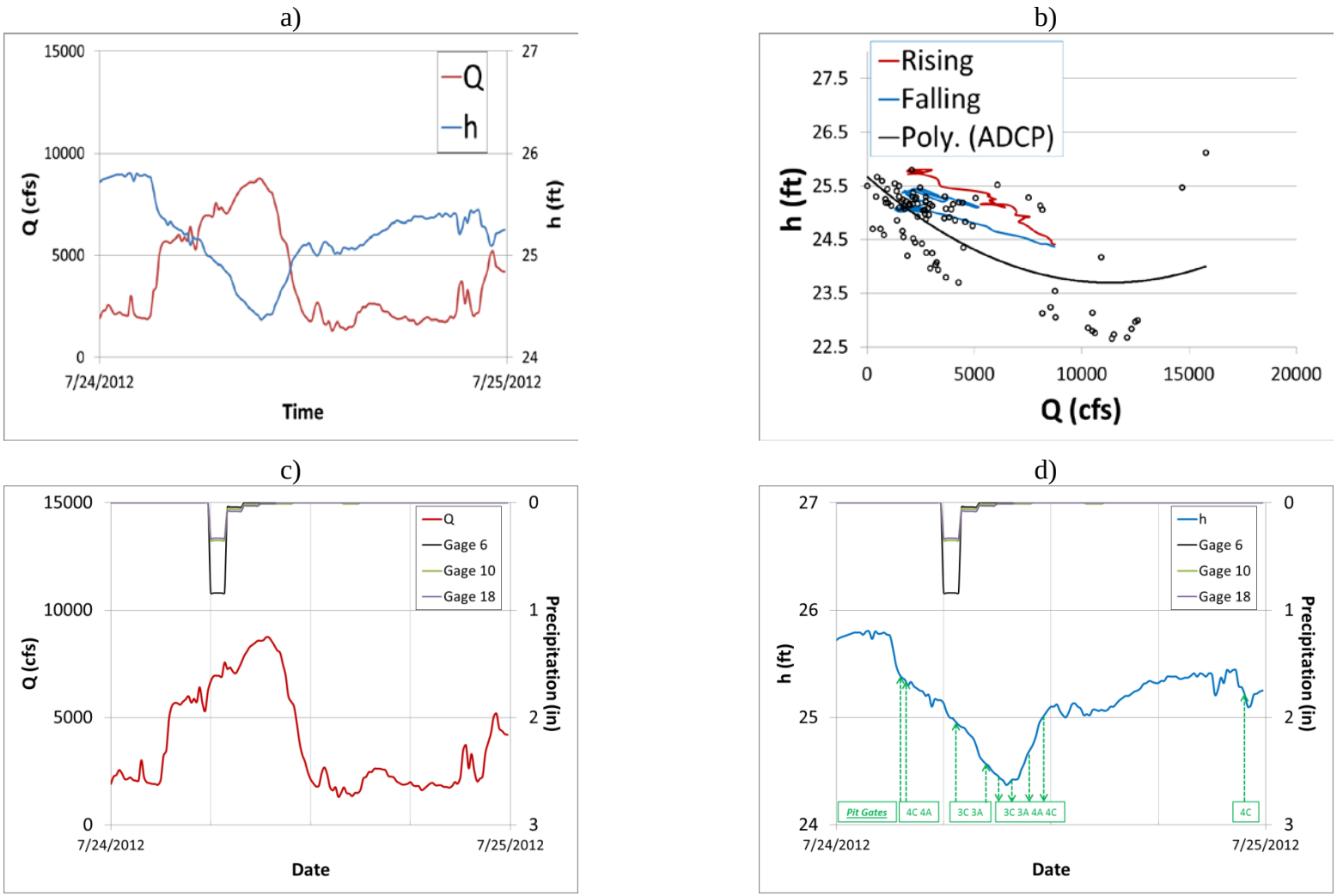

Figure 14 The July 24, 2012 storm (Event 3 in Table 3) as described by precipitation, control structure sequencing, and streamflow recorded at the Lemont gaging station: a) stage and discharge time series; b) stage-discharge relationship; c) time series of discharge and precipitation; d) time history of precipitation, stage, and timing of the operation at the Lockport controlling structures

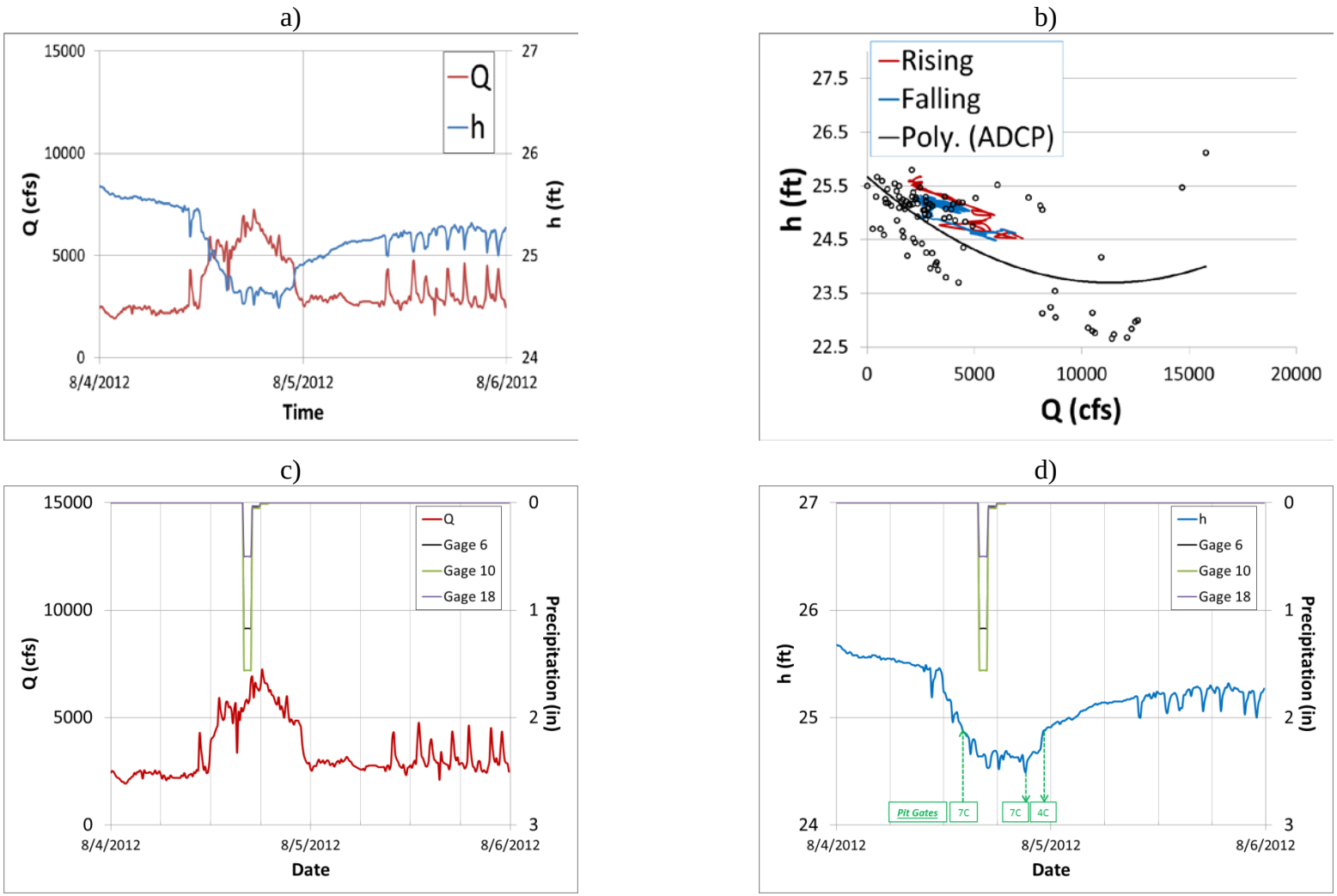

Figure 15 The August 4-5, 2012 storm (Event 4 in Table 3) as described by precipitation, control structure sequencing, and streamflow recorded at the Lemont gaging station: a) stage and discharge time series; b) stage-discharge relationship; c) time series of discharge and precipitation; d) time history of precipitation, stage, and timing of the operation at the Lockport controlling structures

While there is no USGS-established h-QRC for Lemont station built with conventional approaches (E.g. Rantz et al. 1982), we constructed an h-QRC surrogate using the available direct discharge measurements acquired during drawdown events. The regression line through these points, labeled Poly (ADCP) in Figure 16, provides a steady (one-to-one relationship) h-QRC that it is used herein to substantiate other relevant aspects of the I-VRCs. Specifically, Figure 16.b. shows differences in the absolute magnitude of the discharges estimated with the two RC alternatives. A subsequent estimation of the flow volumes passed through Lemont gaging station using the two RC approaches results in a 27.6 billion cfs for the I-VRC and 23.1 billion cfs for h-QRC. These results suggest that not only that the I-VRC captures more accurately the non-unique relationship for the rising and falling limbs of the hydrographs but it also provides less flow volumes than those estimated by the h-QRC. Due to its importance for the overall goal of the LMDA annual reports, this finding is essential and requires further confirmation through well-documented flow events and types of flows occurring in the CSSC system.

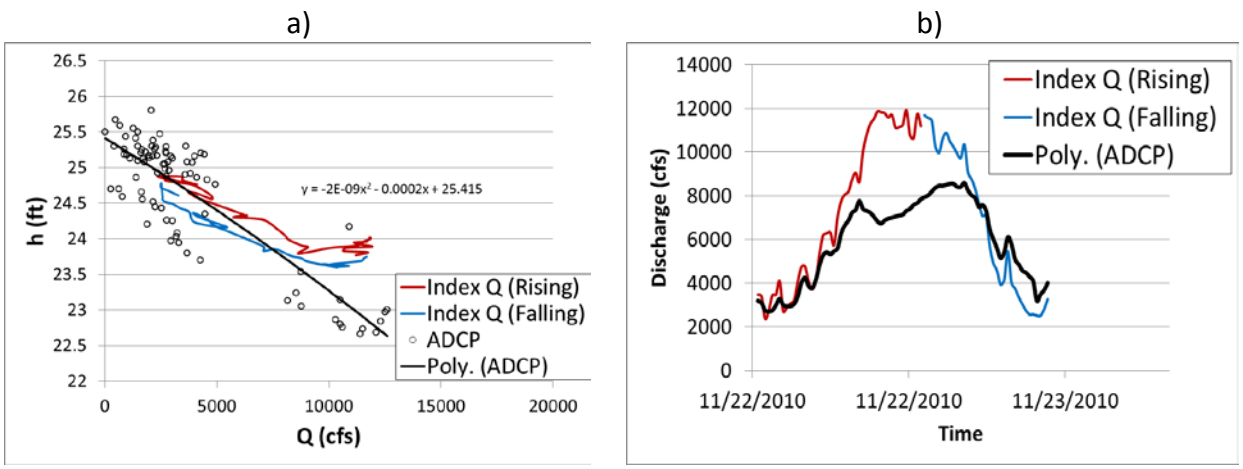

Figure 16 Comparison of the h-QRC surrogate with I-VRC discharge estimates: a) h-QRC obtained using the available direct discharge measurements during drawdowns; b) comparison of discharge time series obtained with the two alternative RCs.

4.3.2. Drawdowns combined with large storm events

Drawdowns are always carried out by MWRDGC in anticipation of the large flows produced by storm events. While Section 4.3.2 analyzes only the drawdown type of flows in the system, this section scrutinized in a similar pattern drawdown followed by inflows from storm runoff. Jackson et al. (2013) reports two such events: the storm on July 22-26, 2010 (identified as Cases 1 and 2 in Table 3) and the storm on August 26-28, identified as Event 2 in Table 3). Both PH and LCW gates were used for controlling the flow according to the timing provided in Tables 8 and 9. The stage and discharge time series, along with the precipitation recorded at gages 6, 10, and 18 in the basin and the sequencing of control structure operations during these two events are illustrated in Figures 17 and 18, respectively. The arrows pointing upward identify opening of the gates; the arrows point downward identify the closing of the gates.

Table 8 Timing of the operations at the Lockport controlling structures for the July 22-26, 2010 storm event (Case 1 in Table 3)

		Generators				Pit Gates			Controlling Works Gates		
Date	**Time**	**Gen#**	**Flow**	**Gen#**	**Flow**	**Pit**	**Time gate**		**CWorks**	**Time gate**	
			cfs		cfs	**Gate#**	**Opened**	**Closed**	**Gate#**	**Opened**	**Closed**
7/23/10	MID	ONE	1500	TWO	1500	3C	11:50 PM	left opened			
FRI	4:30 AM	ONE	1000	TWO	1000	4A	11:50 PM	left opened		NONE	
	8:40 AM	ONE	0	TWO	1000	4B	10:05 PM	left opened			
	4:40 PM	ONE	0	TWO	2000						
	6:30 PM	ONE	1500	TWO	1500						
	7:40 PM	ONE	2000	TWO	2000						
7/24/10	MID	ONE	2000	TWO	2000	3A	12:08 PM	left opened	ONE	1:00 AM	left opened
SAT	12:15 AM	ONE	1500	TWO	1500	3B	1:30 AM	left opened	FOUR	1:00 AM	left opened
	11:59 PM	ONE	1500	TWO	1500	3C	MID	left opened	FIVE	1:00 AM	left opened
						4A	MID	left opened	SIX	1:00 AM	left opened
						4B	MID	left opened	SEVEN	1:00 AM	left opened
						4C	12:20 AM	left opened			
7/25/10	MID	ONE	1500	TWO	1500	3A	MID	8:43 PM	ONE	MID	8:45 PM
SUN	11:59 PM	ONE	1500	TWO	1500	3B	MID	7:45 PM	FOUR	MID	7:30 PM
						3C	MID	8:43 PM	FIVE	MID	7:20 PM
						4A	MID	left opened	SIX	MID	7:00 PM
						4B	MID	left opened	SEVEN	MID	6:50 PM
						4C	MID	7:45 PM			
7/26/10	MID	ONE	1500	TWO	1500	4A	MID	4:45 AM			
MON	6:00 AM	ONE	1900	TWO	1900	4B	MID	6:00 AM		NONE	
	8:45 AM	ONE	2300	TWO	0						
	2:11 PM	ONE	1200	TWO	1200						
	11:35 PM	ONE	1500	TWO	1500						

Table 9 Timing of the operations at the Lockport controlling structures for the August 26-28, 2012 storm (Event 2 in Table 3)

		Generators				Pit Gates			Controlling Works Gates		
Date	**Time**	**Gen#**	**Flow**	**Gen#**	**Flow**	**Pit**	**Time gate**		**CWorks**	**Time gate**	
			cfs		cfs	**Gate#**	**Opened**	**Closed**	**Gate#**	**Opened**	**Closed**
8/26/12		ONE	0	TWO	0	3A	closed				
SUN						3B	7:35 PM	left opened		NONE	
						3C	7:35 PM	left opened			
						4A	9:10 AM	left opened			
						4B	closed				
						4C	6:45 AM	left opened			
						7A	9:35 PM	left opened			
						7B	MID	left opened			
						7C	8:35 PM	left opened			
8/27/12		ONE	0	TWO	0	3A	closed				
MON						3B	MID	7:45 AM		NONE	
						3C	MID	10:45 AM			
						4A	MID	3:10 PM			
						4B	closed				
						4C	MID	left opened			
						7A	MID	7:10 AM			
						7B	MID	7:10 AM			
						7C	MID	7:45 AM			

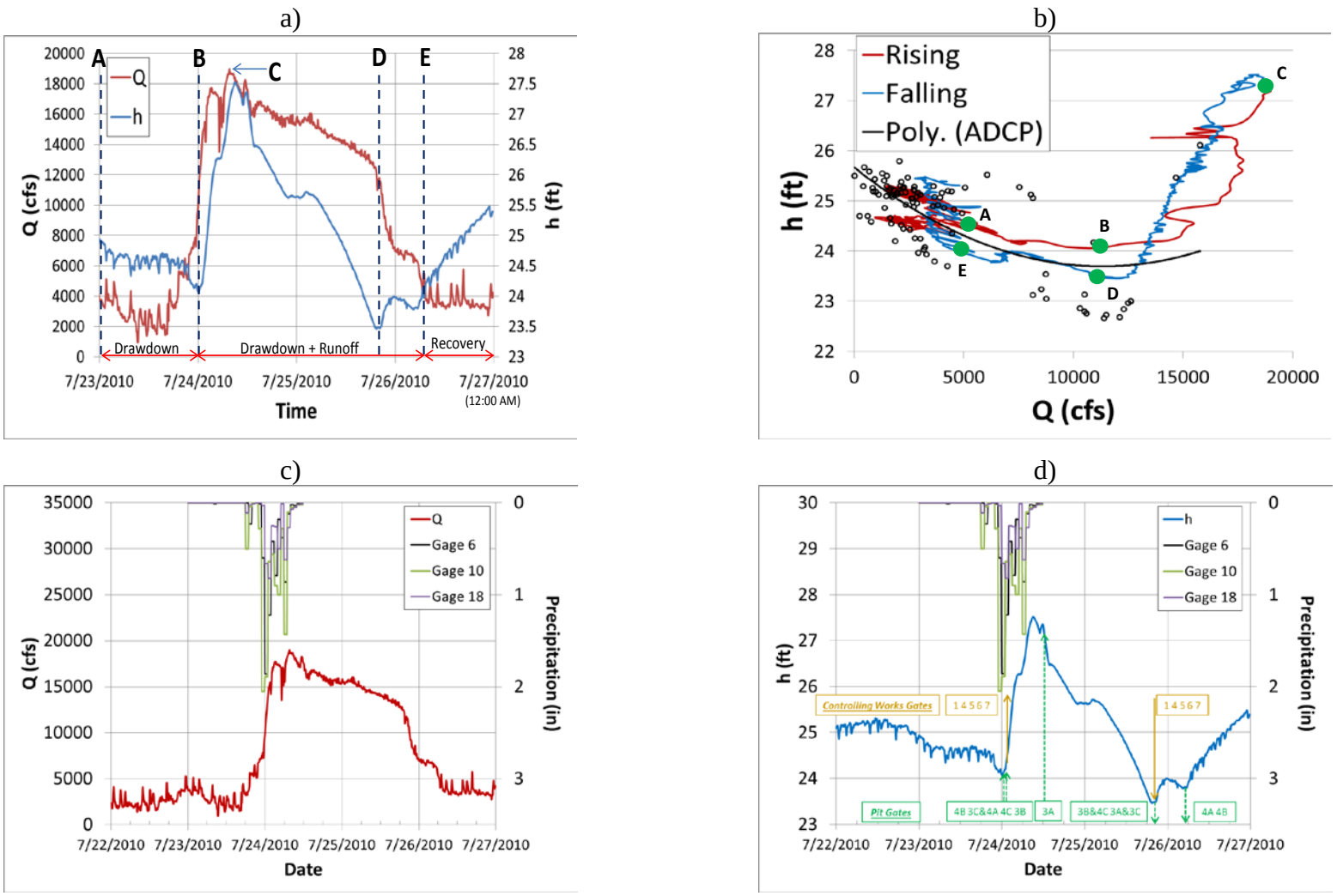

Figure 17 The July 22-26, 2010 storm event (Case 1 in Table 3) as described by precipitation, control structure sequencing, and streamflow recorded at the Lemont gaging station: a) stage and discharge time series; b) stage-discharge relationship; c) time series of discharge and precipitation; d) time history of precipitation, stage, and timing of the operation at the Lockport controlling structures

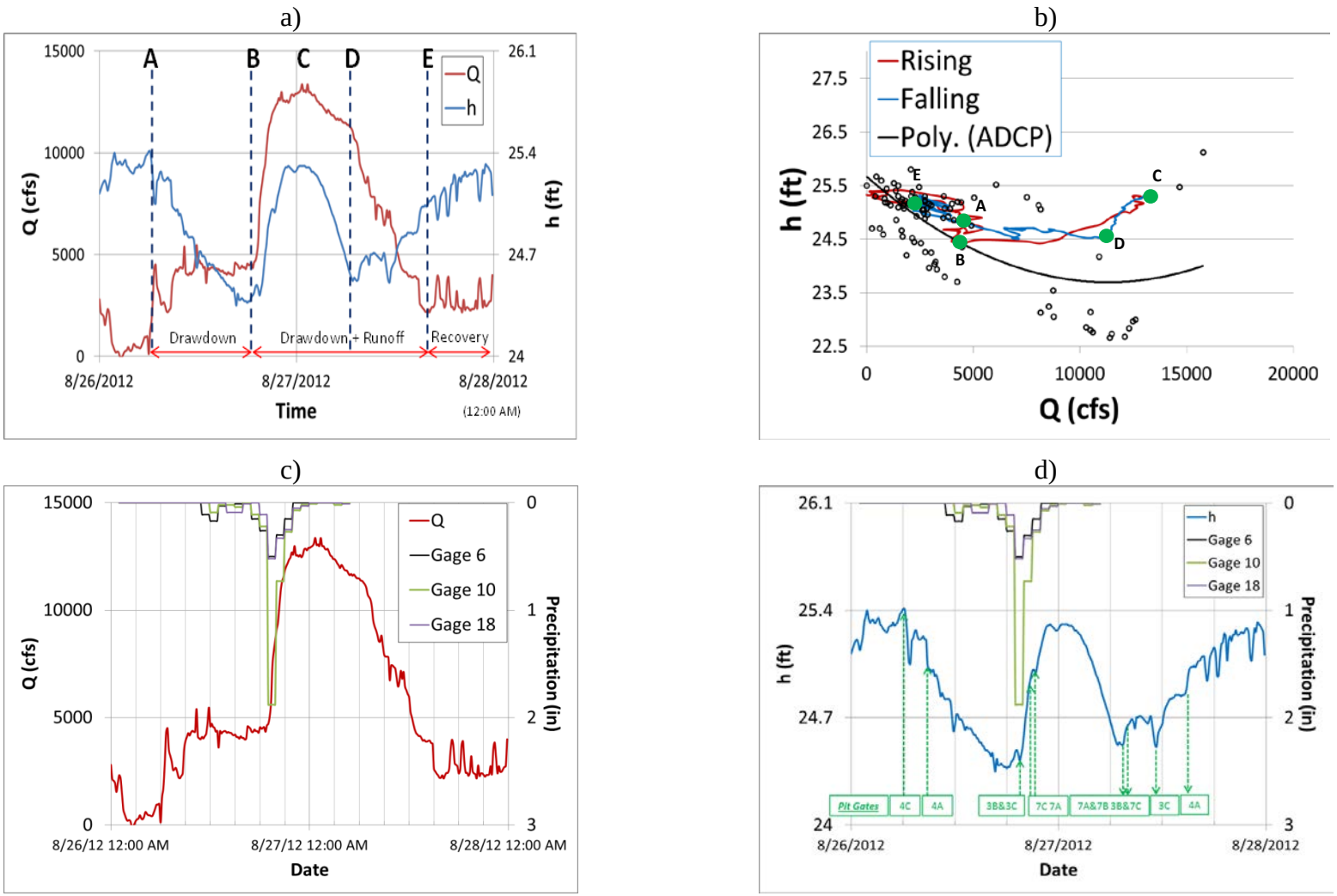

Figure 18 The August 26-28, 2012 storm (Event 2 in Table 3) as described by precipitation, control structure sequencing, and streamflow recorded at the Lemont gaging station: a) stage and discharge time series; b) stage-discharge relationship; c) time series of discharge and precipitation; d) time history of precipitation, stage, and timing of the operation at the Lockport controlling structures

While Figures 17.a), c), d) and 18.a), c), d) do not reveal immediate notable features in the time series, the h-QRC type of plots illustrated in Figure 17.b) and 18.b) reveal notable features that are quite different from the stage-discharge relationships plotted in Figures 12.b), 13.b), 14.b), and 15.b). Specifically, the storm events on July 22 and August 26-28, 2012 display long upward tails corresponding to the signature of the inflow hydrographs propagating through the Lemont gaging station. Traces of this upward pattern in the h-QRC are also found in clusters O1 and O4 of the plots in Figure 7. It can be observed that the h-QRC representation of the variables display a non-unique relationship throughout the lifetime of the event. Moreover, the rising and falling limbs orientation is changing sign: from counter-clockwise during the drawdown to clockwise during the runoff inflow propagation.

Using these overall trends, we employ Jackson's (2009 - personal communication) approach to identify the main moments of the flow events. According to this approach we distinguish the following sequence of dominant flows in the system (see Figures 17.a) and 18.a)): drawdown, drawdown plus runoff; flow recovery. The points separating these regimes are labeled as A, D, and E in those figures. In addition, we marked with B and D the peak and lowest discharges during the event. These critical points are plotted in Figures 17.b) and 18.b). The arrangement of the points suggests that points A, B, D and E visualize the drawdown from inception to recovery. In between these points, there is a time period dominated by the effect of inflow in the channel indicated by the sequence of points B, C, and D. This part of the h-Q plot resembles well the typical hysteretic curves displayed in Figure 1. They also confirm one again that the I-VRC discharge estimates are more apt in capturing the flow dynamic with unique relationships for the rising and falling limbs of the hydrograph. Another feature of these plots is that they substantiate the relevance of the 12,000cfs threshold discharge value corresponding to the quasi-steady flow in the channel.

4.4. Analytical Investigation of Hysteresis in CSSC

The flow events analyzed in Sections 4.3.1 and 4.3.2 reveal that the drawdown is practically present in most of the unsteady flow situations in CSSC system. The drawdown presence is unfortunate for the present study as the analytical tools proposed for conducting the study are best applied to single events propagating as flood waves through geometrically uniform channels, as demonstrated in Section 3. During the USGS-USACE-IIHR July 2013 meeting it was concluded that such flow situations are rare (if at all present) in the CSSC waterscape. Even if the perturbations are produced by runoff inflows without triggering drawdowns at Lockport, the unsteady flow pulses generated in CSSC and Cal-Sag channels upstream from Lemont will superpose by the time they arrive at the gaging station. This combination of unsteady flow pulses cannot be either treated accurately with conventional methods for correction of the hysteresis effects such as Jones or Fread methods.

Lacking a proper type of flow for implementing the analytical tools described in Section 3, attempts were made to apply Fread's (1975) method to the unsteady flow produced by the

combination of drawdown and runoff inflow at the Lemont gaging station. The event selected for illustration purposes is the July 22-26, 2010 storm (Events 1 and 2 in Table 3).

Fread analytical solution (equation 3) is applied for Cases 1 and 2 in Table 3 for the runoff-dominated hydrograph, i.e., discharges greater than 12,000 cfs whereby the flow is controlled by channel governing equations (rather than section control). The channel bed slope (S_0) for the Lemont gaging station was determined as 0.00005 based on the survey conducted in 1896 by Charles Shattuck Hill (see Figure 19). The initial value of the Manning's *n* was set at 0.0358 as obtained through numerical model calibration in Jackson et al. (2013) study. A value of 0.023 for Manning *n* is obtained by assuming that the estimated channel bed slope of 0.00005 is reliable and in conjunction with discharges obtained from the I-VRC applied at Lemont station. This latter value was further used in the analysis. It is worth mentioning that the value of Manning's *n* does not affect the thickness of the hysteretic loop, rather its positioning in the h-Q coordinates. The other inputs for the Fread's equation were derived from the directly measured variables at the Lemont gaging station. The results of Fread's method are plotted in Figure 20 in stage-discharge coordinates.

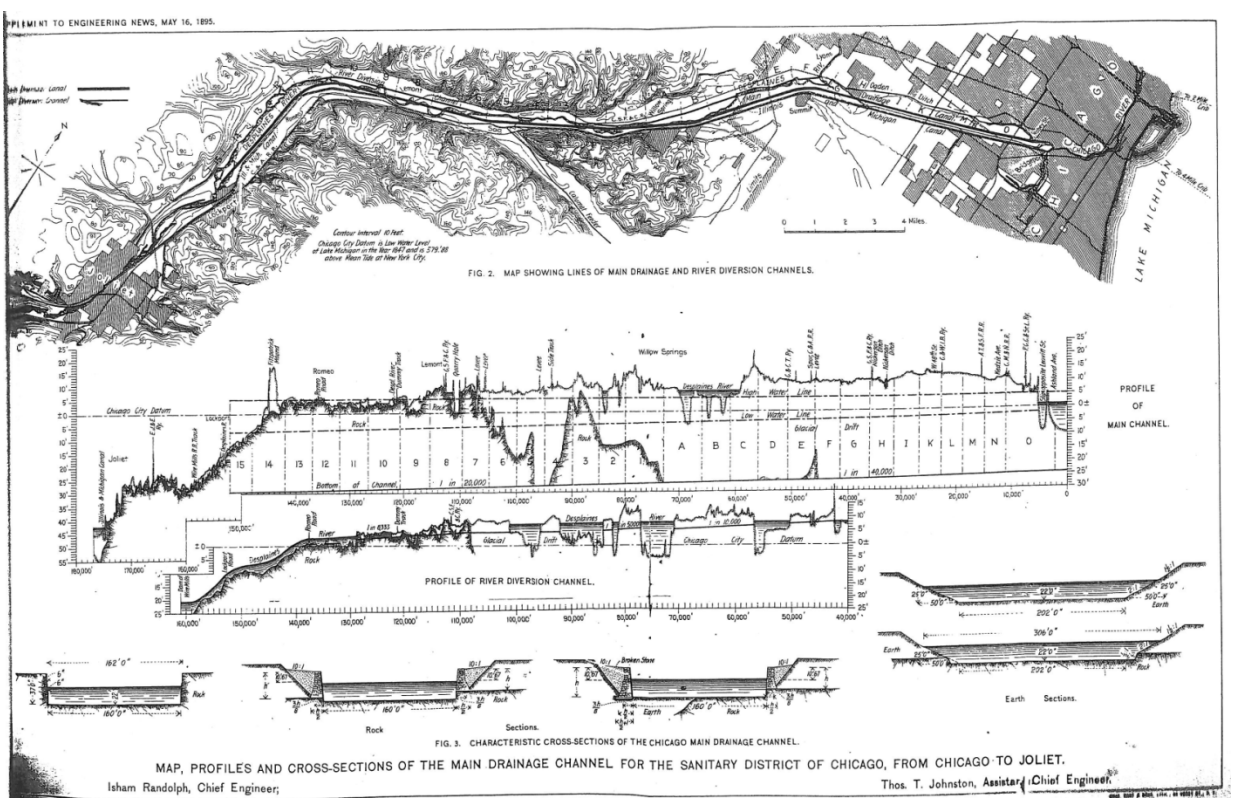

Figure 19 Streamwise profiles and cross sections for the main stem of the CSSC system (Source: Charles Shatuk Hill, 1986)

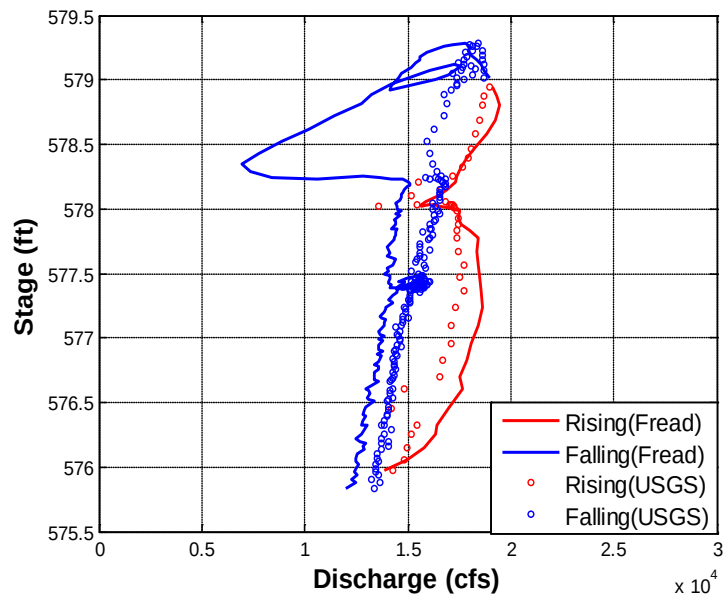

Figure 20 Comparison between discharges estimated with I-VRC at Lemont and Fread's method for S_o=0.00005 and n=0.023

Solid lines in Figure 20 represent estimated stage-discharge relationship based on Fread (1975) equation. The hollow circles represent computed discharges based on I-VRC at Lemont gaging station. Inspection of the two curves plotted in Figure 20 show that Fread equation results in a thicker (over-estimation) of the hysteretic loop. The authors attribute this difference to the combined effect of the runoff and drawdown waves. The first is well described by Fread equation while the unsteadiness associated with the drawdown wave was not considered in the Fread's equation input data (and cannot be obtained from the available records). With respect to Equation 3, this statement translates in stating that the third term (local acceleration) inside the square bracket of the equation has negative value (-) while the second term (pressure term) is positive (+) on the rising limb of the event. On the falling limb, the third term of in the square bracket of the equation becomes positive (+) while the second term becomes negative (-).

Overall, it can be concluded that Fread's method indicates a well differentiated hysteretic loop in the h-Q representation of the flow variables at the Lemont station confirming the hysteresis presence. The fact that the I-VRC discharge estimates also display different paths for the rising and falling limbs of the hydrograph is a confirmation of the hysteresis presence. The different thickness of the hysteresis loops is attributed to unsteady effects not accounted for in Fread formula (Equation 3). The effect of the missing data can be also by explained using the terms in Equation 3. These preliminary results are not exhaustive but serve well to illustrate the capabilities of the analytical tools to substantiate hysteresis. Actually, there are many other case studies that have illustrated good agreement of the Fread's method with directly discharge measurements in various stream sizes and storm intensities (Lee, 2013). Given the limited data available for the study to properly describe the combination of unsteady effects propagating at Lemont gaging station during storm events, it is suggested to further this type of investigations in conjunction with adequately acquired data for the analysis.

4.5. Additional Considerations on I-VRCs

A key variable in constructing I-VRCs is the vertical velocity distribution which is typically assumed to obey distribution laws for steady, uniform open-channel flows. Laboratory and field experiments available in the literature show, however, that during unsteady flow the shape of the vertical velocity profiles for steady flow are affected by hysteretic effects. Specifically, the rising and falling stages of a storm event propagating through a test section follow distinct relationships. For illustration purposes result of laboratory studies and field measurements are provided in Figure 21. The figure illustrates that the stage-mean velocity relationship displays a hysteretic behavior (21.a)); the shape of the vertical velocity distribution and the flow depth are function of the acceleration/deceleration phase during the event propagation (21.b)).

It is the combination of the change of the velocity profile and depth that will eventually determine the uncertainty in discharge estimation using the steady versus unsteady I-VRC approach. There is field data documenting that hysteresis occurs not only in the stage-discharge relationship but also in the index-velocity RCs, as illustrated in Figure 21.c), where it can be observed that the RCs display distinct curves for the rising and falling phases of the storm propagation compared to the steady RC. It also can be noted from in this figure that the significance of hysteresis is more prominent for large events.

With the above considerations in mind, we applied a sensitivity analysis to illustrate the influence of the location of velocity for the H-ADCP in the vertical for the Lemont gaging station. The data used in the analysis is taken from the Jackson et al. (2012) study and reproduced herein for convenience in Figure 22.a). Among other results of interest in the present context are the average profiles acquired over 4 years with Acoustic Velocity Meter (AVM). The analysis led the authors to conclude that the long-term time-averaged data indicate the vertical profiles profile in the CSSC near Lemont replicate the logarithmic profile. The one-sixth power law does not perform well, displaying deviations for higher flow velocities (> 3 ft/s). Using data described by the logarithmic law, we developed power laws corresponding to ranges of velocities that may occur during one storm event propagating through the station. The derived power laws are provided in Table 10.

Using the obtained velocity distributions we simulated the corresponding index-velocity RC for H-ADCP located at three vertical positions, i.e. z= 8.06 ft, z = 13.5 and z= 18.8 ft. These positions correspond to the location of the AVMs in the cross-section. The results plotted in Figure 22.b) shows that the RC is not the same for the three vertical locations, showing a monotonic trend with the change in the location of the H-ADCP. Obviously, this will impact the accuracy of the discharge estimates during the propagation of the storm wave where for the largest ones it is expected to experience changes in stages up to 4 ft (see Figure 17.a)). The findings calls for further studies to establish the optimal location of the H-ADCP in the vertical to preclude biases in the I-VRC estimates, especially for high velocity flows.

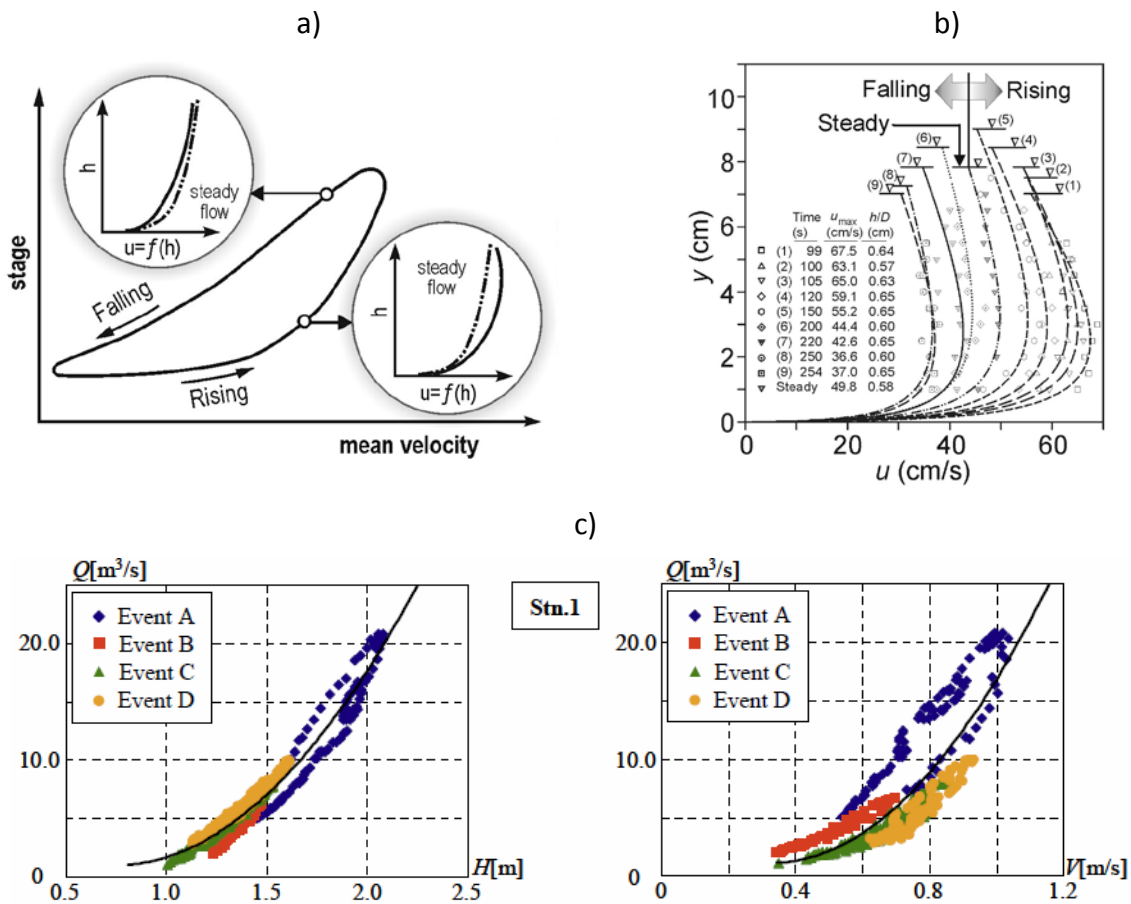

Figure 21 Experimental evidence illustrating hysteresis in I-VRC: a, b) laboratory studies by Graf & Qu (2004) and Tu et al. (1995), respectively; c) field data by Nihei & Sakai (2006)

Table 10 Power law used in conjunction with the AVM for estimating the depth-averaged velocity at Lemont gaging station

	All data		u_path2 < 1.0 ft/s		u_path2 > 1.0 & < 3.0 ft/s		u_path2_>3.0 ft/s	
	Z, ft	U, ft/s	Z, ft	U, ft/s	Z, ft	U, ft/s	Z, ft	U, ft/s
	8.1	0.69	8.1	0.57	8.1	1.21	8.1	3.47
	13.5	0.75	13.5	0.63	13.5	1.28	13.5	3.74
	18.7	0.80	18.7	0.67	18.7	1.34	18.7	3.87
Power laws used to estimate mean velocity from AVM readouts	$Z=67.5V^{5.7}$		$Z=159.7V^{5.3}$		$Z=1.76V^{8.1}$		$Z=0.0007V^{7.5}$	
Mean Velocity (ft/s) (Z=15ft at 0.6D)	0.77		0.64		1.30		3.80	

a)

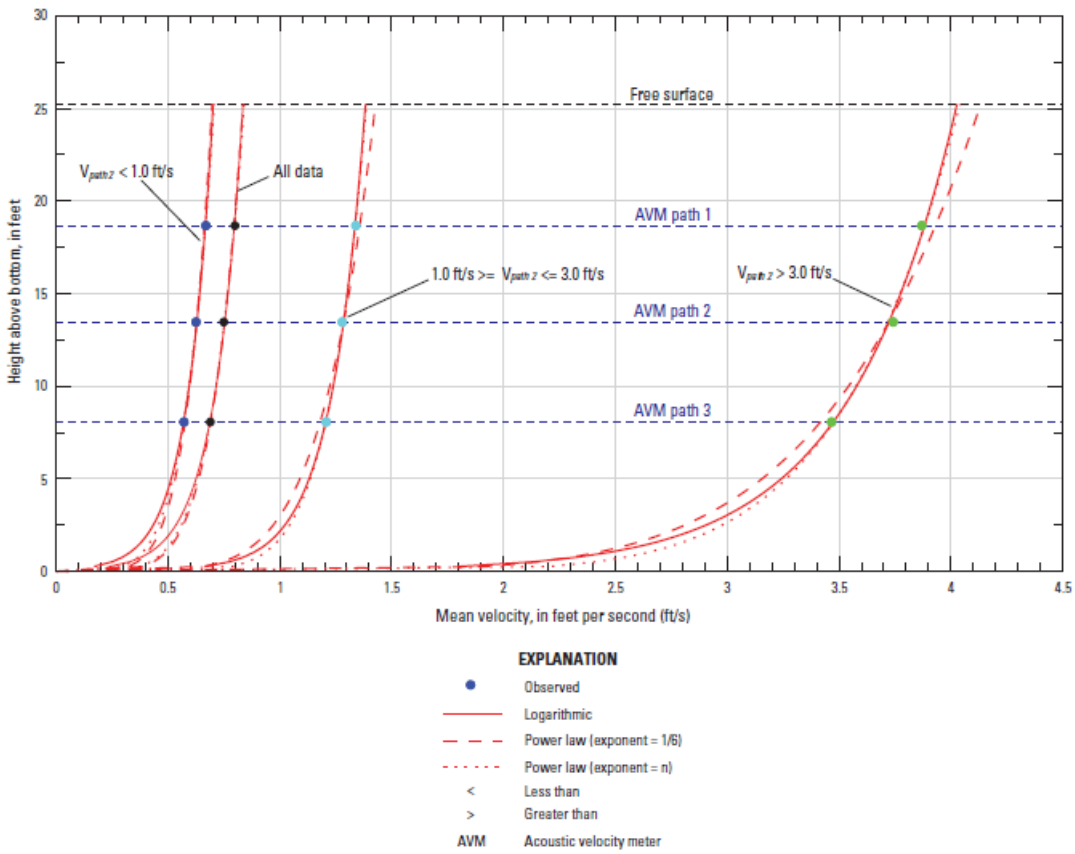

b)

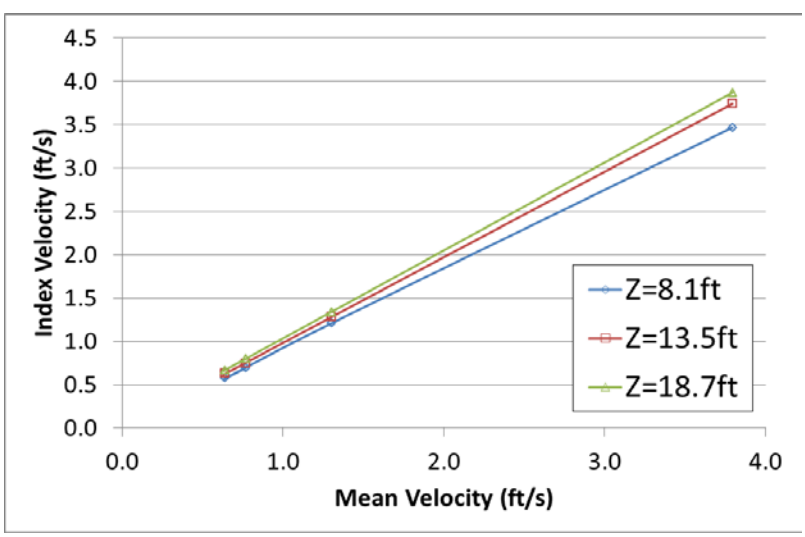

Figure 22 Influence of the H-ADCP location for I-VRC at the Lemont gaging station: a) typical vertical velocity distribution laws for various ranges of velocities (Jackson et al. (2012); b) influence on the I-VRC with the change in the vertical location of the H-ADCP.

4.6 Discussion and Findings

The overarching goals of this study are to substantiate the impact of hysteretic behavior on the index-velocity rating curves (I-VRCs) and evaluate their feasibility for accurate estimation of discharges. The approach and analytical tools used to achieve the study goal entail:

a) Use of discharge estimate datasets provided by the I-VRC protocol established by USGS monitoring program for the Lemont gaging station
b) Representing the I-VRC estimates in stage-discharge coordinates to observe and compare the CSSC data with results previously reported in the literature
c) Application of the Fread (1975) method to CSSC unsteady events for substantiation of hysteresis. The method has proven been extensively used and validated in prior studies. One of these case studies is presented in this report to demonstrate the capabilities of the technique to capture and investigate the hysteresis impact.

A phased approach was adopted for the study, whereby the types of unsteady flows in CSSC were firstly identified. During this phase it was found that the unsteady flow regimes at the Lemont gaging station are the result of the superposition of multiple perturbations (unsteady pulses) in the system upstream and downstream the gaging station. One source of unsteadiness is produced by the controlled drawdowns triggered by MWRDGC in anticipation of the excess inflows accumulated in the system following storms in the Chicago River basin. The drawdowns are typically produced before storm to occur by operating the control structures at Lockport. The extent of the drawdowns is guided by precipitation forecasts.

The other source of unsteadiness in the system consists of inflows produced by runoff collected in the two branches joining upstream of the gaging station, i.e., the CSSC main channel and Cal-Sag channel. The travel time of the runoff inflows is different for the two channels due to the differences in geometry and drainage areas associated with the channel reaches. As a result, the unsteady flows at Lemont gaging station are typically the result of at least three sources of unsteadiness produced at different times depending of the storm characteristics. In addition to these sources, seiche-related flow transients might develop in the CSSC due to the standing waves produced by the three unsteadiness sources in the confined water body of CSSC. The latter effect is not dealt with in this study as it is beyond the initial scope of the project.

Data analysis of the calibration points (i.e., direct discharge measurements) used to construct the I-VRC at Lemont gaging station, time series of the variables associated with storm events investigated by Jackson et al. (2012) and Jackson et al. (2013) studies, along with the implementation of the 1D analytical methods for substantiating the hysteresis lead to the following findings:

- The superposition of the above-described perturbations is expected to diminish the overall impact of hysteresis at Lemont station as the unsteady pulses propagate in opposite directions (i.e., the runoff propagates downstream while the drawdowns propagate upstream) and are out of phase (due to their different time of generation). Confirmation of this hypothesis requires further analysis and customized experiments.

- Most of the calibration points currently used to develop the I-VRC are collected during drawdown episodes. Consequently, the I-VRC might be representative of these types of events and display different trends for other types of unsteadiness in the system.
- Some of the datasets acquired for I-VRC calibration demonstrate that USGS has capabilities to accurately capture the propagation of dynamic events in the system (see for example the dataset acquired on 10/24/2011 – Table 2). Such an operational capability is vital in documenting the impact of hysteresis on the RCs. For this purpose the direct discharge measurements need to be acquired during the whole duration of the unsteady events (i.e., from the beginning to the end) using a sampling frequency commensurate with the lifetime of the unsteadiness.
- The drawdowns and runoff inflows occurring in the system display a hysteretic behavior in the stage-discharge plots (see Figures X.6 to X.12) with distinct relationships for the rising and falling phases of the hydrographs. There is no substantial difference among these phases in the I-VRC. The latter finding leads to the conclusion that I-VRC is capable to better capturing the dynamics of the flow, hence providing accurate discharge estimation in steady and unsteady flow conditions.
- The I-VRC protocol for discharge estimation used Lemont gaging station not only that captures more accurately the dynamics of the flow compared with the steady h-QRC approach but also results in smaller flow volumes passing through the station during unsteady events in comparison with those estimated by the h-QRC (see Figure X.10. This finding is essential in the context of LMDA annual reports where the target is to demonstrate that withdrawal of water from Lake Michigan does not exceed the annual mean discharge of 3,200 cfs.
- Fread's (1975) 1D analytical method used in this study to substantiate hysteresis confirms the presence of hysteretic loops in the h-Q representation of the flow variables at the Lemont station. The method also show good agreement with the discharge estimation during unsteady flow obtained from I-VRC developed for Lemont station.

While highly significant for the present, most of the above-listed findings are qualitative as the present team has had no complete datasets available for thoroughly evaluating the impact of hysteresis on I-VRC. Especially important for these type of analyses are direct discharge measurements acquired during the development of runoff inflow propagation through the Lemont gaging station. In absence of a thorough understanding of the changes in the mean flow structure during the unsteady flow, the only reliable approach to address hysteresis in I-VRC is to adopt the "segmented" rating curve construction that separately accounts for the phases of the flow as recommended by Ruhl and Simpson (2005) for rivers subjected to tides. The obvious segmentation protocol for unsteady flows in inland rivers is to separately construct RCs for the rising and falling limbs of the unsteady flow propagation. This approach is suitable for both I-VRC and h-QRC methods.

5. Conclusions and Recommendations

The flow conditions in the CSSC system are complex due to perturbations generated by the non-uniform variation of the flow in time (unsteady flows) and space (non-symmetric distribution of the velocity in the channel cross section during the propagation of the unsteady events). Despite the potential for its development, the importance of the latter complexity was found non-essential in the recent CSSC investigation conducted by Jackson et al. (2013). Lack of full understanding of the underlying flow processes developing in the system, use of weakly assessed hypothesis in building the RCs, or inadequate measurement protocols may introduce conceptual uncertainties that are difficult to isolate from the other potential uncertainties affecting the accuracy of RCs. In particular, the steady flow equations on which the RCs rely do not consider the effect of temporal and spatial acceleration and the pressure gradient terms that are all involved in the governing equations for propagation of an unsteady flow (Hidayat et al., 2011). Unfortunately, the available literature does not offer useful criteria for defining thresholds to assess hysteresis significance for various river sizes nor for identifying the most appropriate procedures to account for hysteresis at different sites and flow conditions.

The experimental evidence presented in this study proves that the unsteadiness of the flow produce hysteresis in the stage-discharge relationship. The hysteresis is materialized through the non-unique relationships between the plot variables. Moreover, the analysis confirms that the I-VRC method has intrinsic capabilities to better capture hysteresis in comparison with h-QRCs. Some degree of improvement in capturing aspects of unsteady flow by the I-VRC method is expected as it is based on two direct and high-sampling rate measurements acquired simultaneously: stage and index velocity. These velocities can be acquired in a point (e.g., using Acoustic Doppler Velocimeter), along a line (e.g., AVM and vertical or horizontal set ADCPs), or over a surface surface (e.g., Large-scale Particle Image Velocimetry). Given that for a fixed bed channel the stream area is related to stage to a one-to-one relationship disregard if the flow is unsteady or non-uniform, the fact that the actual index velocity is captured as the unsteady flow progresses will lead to two different discharges for the same depth on the rising and falling limbs of the hydrograph even if the index velocity I-VRC is unique. The last observation is not definitive for all CSSC flow conditions as there is experimental evidence that show hysteresis in the I-WRC for some flow situations ((Nihei and Kimizu, 2008; LeCoz et al, 2008; Hoitinik et al., 2009) hence the need for further customized experiments as proposed below.

Based on the findings garnered from the present study, the research team suggests a set of further set of experiments and analyses:

- Acquisition of an increased number of direct discharge measurements above 12,000 cfs in the system for consolidating the calibration points in this flow range.
- Clustering of the calibration points (i.e., direct discharge measurements used to construct and consolidate the I-VRC) according to the phase of unsteadiness propagation, i.e., distinguishing between the rising and falling limbs of inflow hydrographs produced by storms in the watershed. By doing so, one can differentiate the dynamic vs. quasi-steady state of the flow in the CSSC system and to better

substantiate the hysteresis that potentially can develop during unsteady flows (i.e., drawdowns or inflows)in the system.

- Given that the combined unsteady flows developing in the CSSC system cannot be treated with the analytical methods typically used for assessment of hysteresis impact (i.e., 1D flood wave propagation produced by a single unsteadiness source), it is proposed to design customized tests (or identify situations) whereby a single pulse is produced in main stem of the system in absence of drawdowns. The pulse can be generated by a controlled outflow from one of the Sewage Treatment Plant discharging in CSSC system.
- Tracking the single-pulse flows described above or other flow events continuously during the entire cycle (from drawdown inception to the end of the runoff inflow propagation) with a sampling rate commensurate with the lifetime of the event. For example, if the storm duration is 48 hours, direct measurements should be taken at least one per hour; if the storm events is shorter, the frequency should be increased to twice per hour.
- Analysis of the vertical velocity distribution acquired with the vertical ADCP deployed near Lemont gaging station in the summer of 2013 to observe if there are changes in the vertical velocity distribution (i.e., magnitude and shape of the profile) during the rising and falling stage of the hydrographs and also different from the velocity profile for steady, uniform flows.

By carrying out the above-suggested experiments and analyses, the question of the unicity of the index-velocity relationship could be thoroughly addressed and definite conclusions could be drawn regarding the accuracy and significance of unsteady index-velocity rating curves currently in use in CSSC. A good complementary support for the validation of these future inferences is the use of the new calibration curves developed by Straub et al. (2012) for the Lockport Controlling Works (7 sluice gates) and Lockport Powerhouse (9 sluice gates and 2 turbines). Summing up the discharges provided at the end of the CSSC system will provide a good alternative for tracking with sufficient temporal resolution the propagation of the unsteady flows.

References

Birgand, F., Benoist, J.C., Novince, E., Gilliet, N., Saint-Cast, P. and LeSaos., 2005. Mesure des debits a l'aide de debitmetres ultrasonique Doppler- Cas ded petits cours d'eau ruraux. Ingineries, 41, 23-38.

Espey, W.H., Melching, C. and Muste, M., 2009. Lake Michigan Diversion Committee: Findings of the Sixth Technical Committee for Review of Diversion Flow Measurements and Accounting Procedures. U.S. Army Corps of Engineers, Chicago District, Chicago, IL.

Faye, R.E. and Cherry, R.N., 1980. Channel and dynamic flow characteristics of the Chattahoochee River, Buford Dam to Georgia Highway 141. Geological Survey Water-supply Paper 2063, U.S. Government Printing Office, Washington, DC.

Ferrer, C., Moreno, M.L. and Sanchez, R., 2013. The Influence of hysteresis in the development of stage-discharge relationships. Congress SHF Hydrometrie 2013, Paris, France.

Fread, D.L., 1975. Computation of Stage-Discharge Relationships Affected by Unsteady Flow. Water Resources Bulleting, 11(2), 213-228.

Graf, W.H. and Qu, Z., 2004. Flood Hydrographs in Open Channels. Proceedings of the Institute of Civil Engineers Water Management,157, 45-52.

Gunawan, B., 2010. A Study of Flow Structures in a Two-stage Channel Using Field Data, A Physical Model and Numerical Modelling. PhD Thesis Dissertation, The University of Birmingham, UK.

Henderson, F.M., 1966. Open Channel Flow. Macmillan Company, INC, New-York.

Herschy, R.W., 2009. Streamflow Measurements. 3rd edition, Taylor & Francis, New York, NY.

Hidayat, H., Vermeulen, B., Sassi, M.G., Torfs, P.J.J.F. and Hotink, A.J.F. 2011. Discharge estimation in a backwater affected meandering river, Hydrology and Earth System Sciences, 15, 2717-2728

Hoitink, A.J.F., Buschmanm F.A. and Vermeulen, B. 2009. Continuous measurements of discharge from a horizontal acoustic Doppler current profiler in a tidal river, Water Resources Research 45, 1-13

Jackson, P.R., Johnson, K.K. and Duncker, J.J., 2012. Comparison of index velocity measurements made with a horizontal acoustic Doppler current profiler and a three-path acoustic velocity meter for computation of discharge in the Chicago Sanitary and Ship Canal near Lemont, Illinois. USGS Scientific Investigations Report 2011–5205, 42.

Jackson, P.R., Sinha, S., Dutta, S., Johnson, K.K., Duncker, J.J. and Garcia, M.H., 2013. Evaluation of the Potential for Hysteresis in Index-Velocity Ratings for the Chicago Sanitary and Ship Canal near Lemont, Illinois. U.S. Geological Survey Scientific Repoet 2013-5095, 33. available online at http://pubs.usgs.gov/sir/2013/5095.

Kim, D., Muste M. and Weber L., 2005. Development of new ADCP post-processing and visualization capabilities. Proceedings XXXI IAHR Congress, Seoul, Korea.

Knight, D.W., 2006. River flood hydraulics: calibration issues in one-dimensional flood routing models. In: Knight DW, Shamseldin AY (eds) Chapter 18 in river basin modelling for flood risk mitigation, Taylor & Francis, Chichester, 335–385.

Lee, K., 2013. Evaluation of Methodologies for Continuous Discharge Monitoring in Unsteady Open-channel Flows. PhD Thesis Dissertation, the University of Iowa, Iowa City, IA.

Le Coz J., Pierrefeu G. and Paquier A., 2008. Evaluation of river discharges monitored by a fixed side-looking Doppler profiler. Water Resources Research, 44, 1-13.

Levesque, V.A. and Oberg, K.A., 2012. Computing discharge using the index velocity method. U.S. Geological Survey, Techniques and Methods 3–A23, 148. available online at http://pubs.usgs.gov/tm/3a23/.

Lindner, G.A. and A. J. Miller., 2012. Hydraulic Modeling of Stage-Discharge Relationships in Urban Streams. Submitted to Journal of Hydrologic Engineering, 17 (4).

Morlock, S.E., Nguyen, H.T. and Ross, J., 2002. Feasibility of acoustics Doppler velocity meters for the production of discharge records from U.S. Geological Survey stream-flow-gaging stations. U.S Geological Survey, Water-resources Investigations Report, Indianapolis, IN.

Muste, M. and Lee, K., 2013. Quantification of Hysteretic Behavior in Stream Flow Rating Curves. Proceeding of 2013 IAHR World Congress, Chengdu, China.

Nihei Y. and Kimizu A., 2008. A new monitoring system for river discharge with horizontal acoustic Doppler current profiler measurements and river simulations. Water Resources Research, 44. doi:10.1029/2008WRR006970.

Nihei Y. and Sakai T., 2006. Study of river-discharge measurements with a bottom-mounted ADCP. Proceedings River Flow International Conference on Fluvial Hydraulics, Lisbon, Portugal, 6-8 September 2006, Eds. Alves E.C.T.L., Cardoso A.H., Leal J.G.A.B. and Ferreira R.M.L., Taylor and Francis.

Petersen-Øverleir, A., 2006. Modelling stage-discharge relationships affected by hysteresis using the Jones formula and nonlinear regression. Hydrol. Sci. J., 51, 365–388.

Qu, Z., 2003. Unsteady open-channel flow over a mobile bed. PhD Thesis, Ecole Polytechnique Federale de Lausanne, Lausanne, Switzerland.

Ruhl, C.A. and Simpson, M.R., 2005. Computation of discharge using the index-velocity method in tidally affected areas. U.S. Geological Survey, Scientific Investigations Report 2005-5004, Reston, VA, 31.

Sassi, M.G., Hoitink, A.J.F., Vermeulen, B. and Hydayat., 2011. Discharge estimation from H-ADCP measurements in a tidal river subject to sidewall effects and a mobile bed. Water Resources Research, 47, 14.

Schmidt, A.R., 2002. Analysis of Stage-discharge Relations for Open Channel Flows and their Associated Uncertainties. Ph.D. thesis, Univ. of Illinois at Urbana-Champaign, Champaign, IL.

Straub, T.D., Johnson, K.K., Hortness, J.E. and Duncker, J.J., 2012. Control-structure ratings on the Chicago Sanitary and Ship Canal near Lockport, Illinois. U.S. Geological Survey Scientific Investigations Report, 2012–5131.

Rantz, S.E. and others., 1982. Measurement and Computation of Streamflow. United States Geological Survey Water Supply Paper 2175, Vol 1, 2.

USGS. 2011. Exposure time for ADCP Moving-boat discharge Measurements Made During Steady Flow Conditions, USGS Office of Surface Water Technical Memorandum, 2011.08.

Information Transfer Program Introduction

With budget cuts due to federal sequestration in FY2013, Iowa Water Center staff focused efforts on cost-effective methods of information transfer. Emphasis was on info-sharing through the IWC website social media, (including Facebook, Twitter and an e-newsletter) as well as attendance at and promotion of conferences, symposiums, field days, public meetings and other professional events. These efforts simultaneously benefited attendees of the events and the Center by raising public profile of the Center, its efforts, and the Water Resources Research Institutions as a whole.

Iowa Water Center Information Transfer Project

Basic Information

Title:	Iowa Water Center Information Transfer Project
Project Number:	2013IA248B
Start Date:	3/1/2013
End Date:	2/28/2014
Funding Source:	104B
Congressional District:	IA-004
Research Category:	Not Applicable
Focus Category:	None, None, None
Descriptors:	
Principal Investigators:	Richard Cruse, Melissa S Miller

Publication

1. Authors (Melissa Miller, Mohammad Arif Yaqubi, Dean Lemke, Shawn Richmond, Jacqueline Comito, Ann Staudt, Susan Heathcote, Gerald Miller, C. Lee Burras, Yury Chendev, Mostafa Ibrahim, Beth Larabee, Tom Sauer, Ramanathan Sugumaran, John DeGroote, Bernard Conrad, Emily Heaton, Amy Kaleita-Forbes, Matt Liebman, Rick Cruse, S. Elwynn Taylor, Gretchen Zdorowski), 2013, Getting Into Soil and Water, copies available from Iowa Water Center and electronically on water.iastate.edu, pp.38.

2013-2014 Iowa Water Center Information Transfer Project

The Iowa Water Center (IWC) places great importance on the Information Transfer aspect of its 104(b) program. Information Transfer activities achieve multiple goals for IWC: inform consumers about water related issues and research; connect researchers to complementing projects and facilitate collaboration; publicize IWC and its programs and products; and publicize and promote the Water Resources Research Institute Program and U.S. Geological Survey. IWC staff spends a significant portion of their time devoted to organizing, supporting and attending multiple education and outreach activities throughout the year. In addition to events, IWC staff prioritizes maintaining an effect web presence.

Iowa Water Conference

The predominant Iowa Water Center product is the Iowa Water Conference, which was held March 4-5, 2013. The 2013 event was the 7th annual occurrence and had a theme of "H2O: Humans, Science and Oversight." The conference planning committee altered the structure of the 2013 event to discourage attendees from only attending one day of the conference. Conference evaluations were positive; however, attendance at the 2013 conference was down by nearly 100 participants. This decline was likely caused by one of two primary reasons: federal sequestration cut participation for several agencies that attend, and the conference lacked primary marketing efforts that it had in previous years. The conference was still profitable despite the decreased attendance. After the 2013 event, IWC staff and Water Conference committee members identified a plan for improvement for the 2014 event.

One of the most successful features of the 2013 conference was the addition of a track for self-submitted oral research presentations. Researchers from academic, governmental and non-governmental institutions were invited to apply for a 15-minute slot during break-out sessions to present their latest research. Ten researchers presented in 2013; these sessions were well-attended with between 30-60 participants at each session. The Iowa Water Center also hosted a student poster contest during the 2013 Iowa Water Conference, allowing students to present their research and compete for monetary prizes.

Getting Into Soil and Water

The 2013 edition of the *Getting Into Soil and Water* publication, produced with the Soil and Water Conservation Club at Iowa State University, was released at the Iowa Water Conference in 2014. This 39 page publication contains articles from 14 authors, including IWC Director Richard Cruse and previous IWC 104(b) seed grantees Ramanathan Sugumaran and John DeGroote. It is available for download from http://www.water.iastate.edu/content/getting-soil-water. The 2013 publication was distributed to approximately 1500 individuals, including Iowa Water Conference attendees, high school science and vocational agriculture teachers, attendees to the Iowa Environmental 2013 conference, potential students to the Agronomy program at Iowa State University, and handed out at various conferences where IWC was an exhibitor.

Speaking engagements

Iowa Water Center Director Rick Cruse was invited to give several presentations during this reporting period, including:

-The National Adaptation Forum: Adaptation for Landscaping Diversity in Farming and Habitat; April 4, 2013; Denver, CO. "The Soil Conservation Connection."

-Heartland Regional Water Conference; April 15, 2013; Overland Park, KS. "Bioenergy Future Scenarios." Slides available http://www.heartlandwq.iastate.edu/NR/rdonlyres/CEFD89B7-75BF-4857-A137-C7D2477F21C2/172783/Cruse.pdf.

-Forkenbrock Series on Public Policy – Ongoing Impacts and Challenges of the 2008 Floods; May 31, 2013; Cedar Rapids, IA. "Iowa's Changing Climate and Water Run-off: Water runoff trends in Iowa."

-University Council on Water Resources; June 11, 2013; Lake Tahoe, NV. "The nexus: Climate change, global food demand and resource stress."

-Iowa Environmental Council Annual Conference: The Tipping Point; October 11, 2013; Des Moines, IA. "Our Degrading Soil Resource."

-Iowa Learning Farms Field Day; November 12, 2013; Plainfield, IA. "Soil erosion, what are we missing."

-Adapting to Weather Extremes: the Economic Impact in Iowa; December 11, 2013; Des Moines, IA. Panel representation on Agricultural Issues. "The Soil Resource." Slides available http://ppc.uiowa.edu/sites/default/files/cruse_adapting_to_weather_extremes.pdf.

-Iowa State University Extension Crop Advantage Series (three presentations) January 6, 2014 in Sheldon, IA; January 9, 2014 in Mason City, IA; January 10, 2014 in Burlington, IA; "Soil Erosion: How much is really occurring."

-Dallas County Soil and Water Conservation District Commissioners annual awards dinner; February 8, 2014; Adel, IA. "Soil Erosion: How much is really occurring."

Conference planning, exhibiting, and attendance

The Iowa Water Center and its staff assisted in planning and/or exhibiting at various events during the reporting year. At each event, staff identified themselves as Water Center representatives and shared information about IWC and its products. These events include:

-Heartland Regional Water Conference (planning committee); April 15, 2013; Overland Park, KS.
-Conservation Districts of Iowa Annual Conference (exhibitor); September 4-5, 2013; West Des Moines, IA.
-Iowa Environmental Council Annual Conference: At the Tipping Point (exhibitor); October 11, 2013; Des Moines, IA.

-Practical Farmers of Iowa Annual Conference: Well Grounded (exhibitor); January 24-25, 2014; Ames, IA.

IWC staff also attended various meetings throughout the year, including those of watershed organizations and for research projects .

Web presence

The Iowa Water Center recognizes the importance of an effective web presence. To that end, IWC maintained an engaging website, bi-monthly electronic newsletters, and social media accounts on Twitter and Facebook.

Website: During the reporting period, IWC had 3,379 unique visitors to the website (water.iastate.edu). The average session duration was 2:47 with an average 2.61 pages viewed per session.

Newsletter: Newsletters were released the 2nd and 4th Thursday of each month during the reporting period for a total of 24 newsletters. At the beginning of the reporting period, the newsletter had 83 subscribers with a 48% open rate and 27% click-through rate. The last newsletter in the reporting period had 91 subscribers with a 54% open rate and 16% click-through rate.

Twitter: At the end of the reporting period, IWC's Twitter account had 181 followers, gaining 96 followers throughout the year.

Facebook: IWC started the reporting period with 38 likes on Facebook and gained 22 likes during the year, ending at 62. The IWC Facebook page garners the most interaction leading up to and following the Iowa Water Conference.

In the academic summer period, IWC staff hired and supervised a graduate student to operate IWC's web presence. The student was studying agronomy, specifically soil health, but had interest in scientific communication. The student spent ten hours per week learning the different platforms of social media and website management and developed skills in identifying and developing unbiased materials of interest to IWC consumers. Interviews with the student at the conclusion of the summer indicated that the position was a successful partnership. Thus, IWC will continue the Summer Social Media Assistant program into the future as a tool for teaching students about non-traditional methods of scientific communication. The IWC Program Coordinator also provided training on the effective use of social media to additional students in other units on campus.

USGS Summer Intern Program

None.

Student Support					
Category	**Section 104 Base Grant**	**Section 104 NCGP Award**	**NIWR-USGS Internship**	**Supplemental Awards**	**Total**
Undergraduate	1	0	0	0	1
Masters	4	0	0	0	4
Ph.D.	0	1	0	0	1
Post-Doc.	0	0	0	0	0
Total	5	1	0	0	6

Notable Awards and Achievements

In addition to activities reported throughout this document, IWC Director Rick Cruse led the coordination of the chapter on sustainability for the Association of Public and Land Grant Universities Board of Natural Resources Road Map. Through this effort, he directed seven authors from varying institutions in developing a cohesive chapter for a publication that is intended to guide national science, outreach and education efforts. The chapter was published outside of the reporting year, but was written during the reporting year.